

| 1

Dear editor, dear reviewer,

We thank you for your thoughtful comments and the constructive suggestions which were helpful to further improve the manuscript. Attached you can find our comments to those points that require a response, the suggested changes for the revised manuscript in bold print, and a marked-up version of the manuscript. We hope that we successfully addressed each point raised.

All the best

Franziska Koebisch

Anonymous Referee #1

In the paper the effect of rewetting of agricultural peat field on methane formation has been studied by way of pore water and sediment chemistry, isotopic analysis as well as by studying the prevailing microbial community. The authors found evidence that rewetting by fresh water may increase methane emissions due to lack of sulfate and its reduction. In conclusion they suggested using marine water instead of fresh water in waterlogging.

1. The paper is in the scope of BG while it deals with interactions between biological and chemical processes in former cultivated field being subsequently wetland.
2. The authors have used versatile and state-of-art methods and the results are novel.
3. Substantial conclusions have been made. The suppression of methanogenesis by sulfate reduction has been known for a long time. However, in this kind of practical context such substantial conclusions have not been made earlier.
4. The scientific methods are mainly clearly presented, with the exception of pH. Line 123: It was not stated that pH was measured even though the pH device was presented in the same sentence. In addition, the pH was presented in the principal analysis but not discussed. It is suggested that pH will be discussed.

Author's response

- **You are correct, the pH measurements were not mentioned in the method section. Further, the patterns found in pH deserve to be discussed at least briefly.**

Changes in the manuscript

- **pH measurements were mentioned in the methods section, pH values were added in table A1 and the observed patterns in pH are integrated in the description of overall pore water geochemical patterns.**
5. The results are clearly presented and mainly in line with the text and the figures. However, there are discrepancies between the results in Table A1 and Figure 4. Line 268: The authors write that "H₂S concentrations were below detection limit (~1 μM, Fig. 4)". However, according to Table A1 there are higher concentrations (at 10 cm 3 μM, and at 40 cm 2 μM). In addition, the sulfate concentration is suggested to be reported with the same accuracy in Table A1 and Fig. 4. Otherwise the readers of the journal might get confused. Line 274: The same comment as above regarding AVS, and similarly with the other spots.

Author's response

- **We agree, that the description of the H₂S and AVS concentration were not very accurate and that the unit notations presented in Fig 4 (and Fig. 7a and 7c), and Table A1 require harmonization.**

Changes in the manuscript

- **Line 268 (now line 279) was changed to "H₂S concentrations hardly exceeded the detection limit (~1μM, Fig. 4)". inaccurate H₂S and AVS quantity descriptions of other spots were checked thoroughly.**

- **We changed the unit notation of Fig. 4a into ‘mM dissolved S’, the unit notation now corresponds with Table A1 and Fig. 7a and 7c.**
6. The results support the interpretations and conclusions partly but I feel that the equivocal vertical methane concentrations do not clearly support the interpretations and conclusions. For example, along the studied transect the sum of methane concentration till the depth of 40 cm is the highest in spot 2 and the lowest in spot 1. I feel that the topsoil of spot 1 might be aerated occasionally and therefore methanogen formation was the lowest there. The authors do not present any data for water levels in the spots although water saturation is crucial in determining whether the soil is aerobic or anaerobic. In addition, in spot 2 the highest methane concentration is at the depth of 30 cm and there is still some sulfate left in pore water but not any methanogens. On the contrary, at the depth of 30 cm and 20 cm methane concentrations are the lowest in the profile but in these layers there is not any sulfate left. This is contrary to the hypothesis and should be discussed in the text.

Author’s response

- **We agree that patterns in methane concentrations are equivocal. In general, methane concentration pattern should be interpreted with care as methane is a highly volatile gas. Especially at high methane production rates, the indicative value of methane concentration profiles can be easily impaired by erratic ebullitive release. Hence, the observed methane concentration patterns are likely to present a snapshot resulting from the combination of methane production and erratic methane loss but may not be well suited to represent overall patterns in methane production. Therefore, we are very careful concerning the indicative value of single methane concentration data points. Still, we decided to show the methane concentration profiles for the sake of completeness.**
- **Since methanogenesis exerts a strong fractionating effect on CO₂ and DIC is less volatile than methane, we use the $\delta^{13}\text{C}$ values of DIC as indicator for methane production. In concert, with the isotopic composition of methane and the microbial structure, these can provide a comprehensive picture on methane cycling in our study site.**
- **In the current manuscript, we have explicitly qualified the indicative value of methane concentrations and explained why we focus on the isotope composition of methane and DIC instead in line 342f.: “Measured pore water CH₄ concentrations were up to 643 μM with equivocal vertical patterns across spots (Fig. 7a (Fig. 7a), reflecting the methane-specific spatial variability that evolves from small-scale heterogeneity in production and consumption processes and from ebullitive release events (Chanton *et al.*, 1989, Whalen, 2005). The isotope composition of CH₄ (Fig. 7b) and DIC (Fig. 7c) provided a clearer (and probably more robust) indication for patterns of methanogenesis and methanotrophy”.**

- Referee 1 is right in his suggestion that spot 1 is located on slightly higher grounds than spots 2 and 3. Indeed, since the rewetting of the wetland, all spots have been flooded throughout the year, so contemporary water levels should not restrict methane production. In the current manuscript, we have mentioned the hydrological state in line 118f: “At the time of sampling, water depth above peat surface spanned from 9 to 19 cm, which presented the lowest range within the seasonal water level fluctuation”. In fact, lower water levels in the past have, in combination with groundwater flow from the nearby forest catchment, certainly affected peat formation and soil geochemistry at spot 1.

Changes in the manuscript

- We added measured water tables in table A1 and reminded the reader about permanently inundated conditions in the discussion section (line 391). Further, we discussed lower water levels in the past, in combination with mineral inflow from the nearby forest catchment, as possible reasons for the specific geochemistry and microbial community at spot 1 (line 468f.).
7. The description of experiments, the result table and calculations are sufficiently complete and precise to allow their reproduction by fellow scientists.
 8. The authors refer to related work and clearly indicate their own new contribution. The title is clear and reflects the contents of the paper.
 9. The abstract provides a concise and complete summary.
 10. The overall presentation is well structured and clear.
 11. The language is fluent and precise.
 12. Mathematical formulae, symbols, abbreviations, and units are correctly defined and used.
 13. The number and quality of references are appropriate.
 14. The quality of supplementary material is appropriate, but the water table depths in the spots should be presented in a cross-section or in a table.

Changes in the manuscript

- We added water tables in table A1.

Anonymous Referee #2

The manuscript "Sulfate deprivation triggers high methane production in a disturbed and rewetted coastal peatland" by Koebsch et al. is very interesting and informative. The effect of dyking and freshwater rewetting on S and C transformation of a peatland has been studied using various analysis methods. The authors studied four spots with different solid S and sulfate concentrations and discussed the sulfate reduction and CH₄ production and consumption among these sites. They conclude that a replenishment of marine water to dyked wetlands would reduce methane emissions.

Abstract:

Lines 30-32, the word of "suppression" is not accurate since results showed "high contents of labile iron minerals and dissolved ferrous iron at depth of spot 2, coincided with a high abundance of *Thermodesulfobionaceae* at concurrently minor occurrence of *Deltaproteobacteria*. (402-404)".

Lines 34-36: Is that useful to re-exposure of dyked wetlands to natural coastal dynamics since high amounts of sulfate did not interfere with high methane emissions on ecosystem scale?

Author's response

- **Indeed, we think that dissimilatory sulfate reduction at spot 2 is inhibited because we suggest *Thermodesulfobionaceae* present at this spot to utilize mainly ferric iron as electron acceptor (Fortney *et al.*, 2016). This is indicated by the long-term persistence of the brackish sulfate reservoir at concurrently high contents of labile iron minerals and dissolved ferrous iron. This interpretation is stated in detail in line 425 (formerly 394) of the manuscript.**
- **We admit that the used formulations in former lines 34-36 might have been confusing for the reader.**

Changes in the manuscript

- **'suppression' in line 29 (formerly lines 30-32) is replaced with 'inhibition'.**
- **we added an explanation in line 30f.: *However, as the occurrence of sulfate was confined to the peat layers below 30-40 cm, it did not interfere with high methane emissions on ecosystem scale.***

Introduction

Lines 46-47: "dissimilatory sulfate reduction of dissolved organic matter (DSR)" changed to "dissimilatory sulfate reduction (DSR) of dissolved organic matter".

Line 63: Wrong left parenthesis. {Wen & Unger, 2018}.

Line 75: Lack of "."

Author's response

Text mistakes were corrected accordingly.

Material and Methods

Lines 105-107: Please check the parenthesis and should not be set in italic.

Line 159: Please define the abbreviation of DOC. It seems that the results of stable carbon isotope ratio of DOC was not presented in the result or discussion.

Line 160: Ertl and Spitzzy (2004), not list in the Reference. Please check the manuscript completely.

Lines 168, 285, 308: Böttcher et al. (2007), not list in the Reference. Please check the manuscript completely.

Line 185: Please clarify DNA or RNA? Since only DNA has been extracted from samples, hence, I suggest to delete RNA.

Line 191: Please define the abbreviation of AVS. e.g. (acid volatile sulfur).

Lines 196-199: What's the meaning of "reactive iron"? How to detect the dissolved Fe and the valence of Fe (Fe(II) or Fe(III))?

Line 200 indicated the extracted iron fraction consists of iron(III) oxyhydroxides and iron(II) monosulfides, was the dissolved Fe(II) also existed (Heronet al., 1994. Speciation of Fe(II) and Fe(III) in contaminated aquifer sediments using chemical extraction techniques. Environmental Science & Technology, 28(9), 1698-705.)? The reference of Canfield, 1989 was not list, please check.

Line 200: Stookey (1970), not list in the Reference.

Line 223: "Sequence raw reads" changed to "Raw sequence reads".

Lines 229-230: Clarify the number of the sequence. 18.500 or 18,500? 12.500 or 12,500?

Author's response

- **Reactive iron is considered here as the sum of those iron fractions that still may react with dissolved sulfide. The applied analytical extraction scheme extracts the sum of remaining iron(III) oxyhydroxides and acid volatile sulfide (AVS, essentially FeS) as well as a very minor contribution from dissolved Fe²⁺ in the pore water (Canfield, 1989). No further quantification of different di- and trivalent iron was carried out.**

Changes in the manuscript

- **The meaning of 'reactive iron' was specified in the method section and the reference Canfield 1989 was added in the reference list.**
- **Text mistakes were corrected accordingly, references were checked, abbreviations were defined.**

Results

Lines 240-241: Lack of "). Please check the manuscript completely.

Lines 271-272: What's the detailed detection method of organic-bond S and where is the data of organic-bond S? Is it in the Figure 4 or TABLE A1? The note in the Figure 4 indicated that the solid residual S fraction is suggested to present primarily organic-bond S. However, the content (0.2 to 1.6%dwt) in spot 1 (lines 271-272) seems inconsistent with Figure 4b (far less than 1%dwt). What's the relationship between TABLE A1 and Figure 4 and 5?

Lines 291, 322: Similar question to the line 271-272. Table A1 seems to address the organic-bond S content (0.2 to 1.6 %dwt). What's the difference between orgS in Table A1 and solid residual S in Figure 4b? Please clarify.

Lines 298-299 and 392-393: It seems inconsistent to Figure 4a. In the figure, the 1 mM sulfate concentration was appeared at 60cmbsf of spot 3, however, the relative abundance of Chloroflexi was missed at 60cmbsf of spot 3. Please clarify.

Lines 331-332: How to understand the role of DIC in methane production and consumption?

Line 340: Whiticar (1986), not list in the Reference. Please check.

Author's response

- In our study we assume that the solid residual S fraction corresponds primarily to organic-bond S. Unfortunately, we have made a mistake in the residual S fraction values in table A1. The mistake will be corrected. However, this will not affect the main patterns and results of our work.
- We are sorry that the depth indications for spot 3 in Fig. 4d are shifted. The text is correct as the 40% relative abundance of Chloroflexi of the class Dehalococcoidetes represented the dominating bacterial group at the 1 mM sulfate concentration at 60 cm depth of spot 3.
- The formation of methane is a highly fractionating process and results in CO₂ that is considerably enriched in ¹³C compared to the starting organic material (~-27‰ in this study) (Whiticar et al. 1986). The isotopic composition of DIC-C can therefore be used as indicator for methane formation in relation to non-fractionating pathways (organic matter fermentation, sulfate reduction, e. g. Corbett et al. 2013). Dissolved methane is highly volatile and especially at high methane production rates, the indicative value of methane concentration profiles can be easily impaired by erratic ebullitive release. Therefore, in this study we decided to use the δ¹³C values of DIC as indicator for methane production. In concert, with the microbial structure, these can provide a comprehensive picture on methane cycling in our study site.

Changes in the manuscript

- the residual S fraction values in table A1 were corrected and then correspond to the organic bond S values in Fig. 4. The text was checked thoroughly for mistakes.
- The depth indications for Fig. 4d spot 3 were corrected.
- Text mistakes were corrected accordingly, references were checked.
- We added a note on the indicative value of δ¹³C-DIC for methanogenesis in the text (lines 343f.).

Discussion

Line 394: "dsrAB" should be italicized.

Line 439: Please define the abbreviation of AOM-SR.

Lines 447-448: In the Figure 7, the obvious increase of δ¹³C-CH₄ and δD-CH₄ ratios were appeared at 50 cmsf of spot 1, however, the relative abundance of methanotrophy was missed at 50 cmsf, hence, how to understand this sentence.

Lines 452-453: Why high sulfate concentration did not interfere with methane production?

Author's response

- Likewise with Fig 4d, depth indications for Fig. 7d are accidentally shifted. The 48% abundance of ANME-2d ranges down to a depth of 50 cmbsf. Accordingly, the observed patterns in $\delta D-CH_4$ and $\delta^{13}C-CH_4$ are consistent with the microbial community structure.
- The remnants of the brackish sulfate reservoir were spatially separated from the zones of methane production: As a result of intense dissimilatory sulfate reduction, residual sulfate persisted only at depth of spot 2 (and in lower amounts at depth of spot 3). Methane production in wetlands is usually confined to the upper peat horizons, and also in our study methane was mainly produced in the upper 30-40 cm. Therefore, we assume that the residual sulfate does not significantly affect methane production. This is stated in line 473f.: *As intense methane production was confined to the upper pore water layers in the entire peatland, it did not interfere with high sulfate concentrations locally preserved as legacy of former brackish impact in the bottom.*

Changes in the manuscript

- Text mistakes were corrected accordingly, abbreviations were defined.
- The depth indications for Fig. 7d were corrected.

Table A1: TS concentrations were inconsistent with dry weight ratios of TS. e.g. why the value of TS percentage is not 0 while TS concentration is 0. What is the meaning of orgS? Ionic valence should be added e.g. Cl⁻, Br⁻, Na⁺.

Author's response

- TS in mmol corresponds to the total dissolved S fraction whilst TS in dry weight ratios corresponds to the solid dissolved S fraction. Anyway, we admit that it would be better to use different abbreviations to avoid confusion.
- Organic S is the residual non-specified solid S fraction.

Changes in the manuscript

- We implemented different abbreviations for solid and dissolved total S.
- As stated above, we corrected the values of orgS so that they are consistent with the quantities represented in Fig 4.
- Ionic valences were added .

Reference

The format of the references should be carefully checked. Non-English language appeared e.g. lines 504-506, 523-524, 602-603. No journal e.g. lines 507-508, 566. Capitalize the first word of journal or not e.g. lines 548, 568, 573, 577. Other format errors in lines e.g. 523-524, 537-538, 546, 585, 624, 628.

Changes in the manuscript

- The reference list was carefully checked.

Figures

Figure 2: Lines 645-646, please rewrite this sentence.

Figure 4: Please unify the formats with Figure 7. e.g. mmol l⁻¹ in Figure 4 while mM in Figure 7. e.g. the name of y-coordinate.

Changes in the manuscript

- Figure captions and axis labels were corrected accordingly.

Author's response reference list

Corbett, J. E., Tfaily, M. M., Burdige, D. J., Cooper, W. T., Glaser, P. H., & Chanton, J. P. (2013). Partitioning pathways of CO₂ production in peatlands with stable carbon isotopes. *Biogeochemistry*, 114(1-3), 327-340.

Fortney, N. W., He, S., Converse, B. J., Beard, B. L., Johnson, C. M., Boyd, E. S., & Roden, E. E. (2016). Microbial Fe (III) oxide reduction potential in Chocolate Pots hot spring, Yellowstone National Park. *Geobiology*, 14(3), 255-275.

Whiticar, M. J., Faber, E., & Schoell, M. (1986). Biogenic methane formation in marine and freshwater environments: CO₂ reduction vs. acetate fermentation—isotope evidence. *Geochimica et Cosmochimica Acta*, 50(5), 693-709.

1 Sulfate deprivation triggers high methane production in a disturbed 2 and rewetted coastal peatland

3 Franziska Koebsch^{1,2}, Matthias Winkel¹, Susanne Liebner^{1,3}, Bo Liu^{4,5}, Julia Westphal⁴, Iris
4 Schmiedinger⁴, Alejandro Spitzky⁶, Matthias Gehre⁷, Gerald Jurasinski², Stefan Köhler², Viktoria Unger²,
5 Marian Koch^{2,8}, Torsten Sachs¹, Michael E. Böttcher⁴

6 ¹GFZ German Research Centre for Geosciences, 14473 Potsdam, Germany

7 ²Department for Landscape Ecology and Site Evaluation, University of Rostock, 18059 Rostock, Germany

8 ³Institute of Biochemistry and Biology, University of Potsdam, 14476 Golm, Germany

9 ⁴Geochemistry and Isotope Biogeochemistry Group, Leibniz Institute for Baltic Sea Research (IOW), 18119 Warnemünde,
10 Germany

11 ⁵Section Marine Geochemistry, Alfred Wegener Institute Helmholtz Center for Polar and Marine Research, Am Handelshafen
12 12, 27570 Bremerhaven, Germany

13 ⁶Institute for Geology, Biogeochemistry Department, University of Hamburg, 20146 Hamburg, Germany

14 ⁷Department of Isotope Biogeochemistry, Helmholtz Centre for Environmental Research UFZ, 04318 Leipzig, Germany

15 ⁸Tropical Plant Production and Agricultural Systems Modelling, University of Göttingen, 37073 Göttingen, Germany

16 *Correspondence to:* Franziska Koebsch (Franziska.koebsch@uni-rostock.de)

17 **Abstract.** In natural coastal wetlands, high supplies of marine sulfate suppress methanogenesis. Coastal wetlands are, however,
18 often subject to disturbance by dyking and drainage for agricultural use and can turn to potent methane sources when rewetted
19 for remediation. This suggests that preceding land use measures can suspend the sulfate-related methane suppressing
20 mechanisms. Here, we unravel the hydrological relocation and biogeochemical S and C transformation processes that induced
21 high methane emissions in a disturbed and rewetted peatland despite former brackish impact. The underlying processes were
22 investigated along a transect of increasing distance to the coastline using a combination of concentration patterns, stable isotope
23 partitioning and analysis of the microbial community structure. We found that dyking and freshwater rewetting caused a
24 distinct freshening and an efficient depletion of the brackish sulfate reservoir by dissimilatory sulfate reduction (DSR). Despite
25 some legacy effects of brackish impact expressed as high amounts of sedimentary S and elevated electrical conductivities,
26 contemporary metabolic processes operated mainly under sulfate-limited conditions. This opened up favourable conditions for
27 the establishment of a prospering methanogenic community in the top 30–40 cm of peat, the structure and physiology of which
28 resembles those of terrestrial organic-rich environments. Locally, high amounts of sulfate persisted in deeper peat layers
29 through the [suppression-inhibition](#) of DSR, probably by competitive electron acceptors of terrestrial origin, for example
30 Fe(III), ~~but~~ [However, as sulfate occurred only in peat layers below 30–40 cm, it](#) did not interfere with high methane emissions
31 on ecosystem scale. Our results indicate that the climate effect of disturbed and remediated coastal wetlands cannot simply be
32 derived by analogy with their natural counterparts. From a greenhouse gas perspective, the re-exposure of dyked wetlands to
33 natural coastal dynamics would literally open up the floodgates for a replenishment of the marine sulfate pool ~~and~~ [therefore](#)
34 constitute an efficient measure to reduce methane emissions.

1. Introduction

Coastal wetlands play an important role in climate change mitigation and adaption as they can efficiently accrete organic sediments, adjust coastal elevations to sea level rise and protect low-lying areas in the hinterland. Further, while freshwater wetlands constitute the largest natural source of the greenhouse gas methane (Zhang *et al.*, 2017), the efficient accumulation of autochthonous C in coastal wetlands comes without the expense of high CH₄ emissions (Holm *et al.*, 2016). Methane is a potent greenhouse gas that is formed as terminal product of organic matter breakdown under strictly anaerobic conditions typically in the absence of electron acceptors other than carbon dioxide (CO₂) (Segers & Kengen, 1998). In coastal environments, methane production and emission are effectively suppressed by sulfate-rich seawaters: methanogens are outcompeted by sulfate reducing bacteria (SRB) for acetate-type precursors and hydrogen (Lovley & Klug, 1983, Schönheit *et al.*, 1982). This shifts the prevailing anaerobic C metabolic pathways from methanogenesis towards dissimilatory sulfate reduction (DSR) of dissolved organic matter (DSR) (King & Wiebe, 1980, Martens & Berner, 1974). In addition, sulfate operates as electron acceptor for anaerobic methane oxidation by a syntrophic consortium of anaerobic methanotrophs (ANME) and SRB (Boetius *et al.*, 2000, Iversen & Jorgensen, 1985). Anaerobic methane oxidation has been specifically described for brackish wetland sediments, but is not exclusively confined to the utilization of sulfate as electron acceptor (Segarra *et al.*, 2015, Segarra *et al.*, 2013).

Human activities such as dyking and drainage place intensive pressure on coastal landscapes with sometimes irreversible impairments of their biogeochemical cycles and ecosystem functions (Karstens *et al.*, 2016, Zhao *et al.*, 2016). Dykes separate coastal wetlands from resupply of seawater, and drainage for agricultural use induces the aerobic decomposition of organic-rich sediments, resulting in substantial CO₂ losses and land subsidence (Deverel *et al.*, 2016, Deverel & Rojstaczer, 1996, Erkens *et al.*, 2016, Miller, 2011). As sea levels are expected to rise, the controlled retreat from flood-prone areas becomes an essential strategy of integral coastal risk management to complement conventional technical solutions such as dyking (Sánchez-Arcilla *et al.*, 2016). Rewetting may re-establish the ability of abandoned coastal wetlands to efficiently accrete organic matter under anaerobic conditions and represents a promising management technique to reverse land surface subsidence caused by drainage-induced peat oxidation (Deverel *et al.*, 2016, Erkens *et al.*, 2016). Moreover, while freshwater wetlands may become methane sources upon rewetting (Franz *et al.*, 2016, Hemes *et al.*, 2018, Vanselow-Algan *et al.*, 2015, Wilson *et al.*, 2009), sulfate-rich seawater could potentially reduce post-rewetting methane release in coastal wetlands. However, recent work on a degraded brackish peatland has revealed high post-rewetting CH₄ emissions (Hahn *et al.*, 2015, Koebsch *et al.*, 2015) and methanogen abundance (Wen *et al.*, 2018) thereby challenging the common notion of coastal wetlands as negligible methane emitters. In fact, dyking and the drainage-rewetting cycle may induce hydrodynamic-hydrological shifts and biogeochemical transformation processes that are so far not well understood. In particular, the transformation and/or relocation of the marine sulfate reservoir in the sediments of dyked wetlands are of vital importance to understand the implications of anthropogenic intervention on coastal wetland biogeochemistry and to better constrain the climate effect of coastal wetland remediation.

68 Here, we investigate the mechanisms that allow for high methane production in disturbed and remediated coastal wetlands.
69 We therefore address the fate of brackish compounds and the emerging S and C transformation processes in a rewetted,
70 freshwater-fed peatland that was naturally exposed to episodic intrusions from the Baltic Sea. In the past, the peatland had
71 been subject to intense human intervention including dyking and drainage for agricultural use. After rewetting by freshwater-
72 flooding, the site turned into a strong methane source. The underlying hydrological and biogeochemical processes were
73 investigated along a brackish-terrestrial transect that spans between 300 and 1,500 m distance from the coastline using
74 hydrogeochemical element patterns, stable isotope biogeochemistry and microbiological analyses.

75 The specific goals were to:

- 76 - retrace the marine legacy effect remaining after dyking and freshwater rewetting in the peat pore space using salinity,
77 the isotope composition of water and a suite of [inert](#) dissolved constituents that may be indicative for the intermingling
78 of brackish ~~or~~ and terrestrial ~~imp~~actwaters
79 ~~— track the distribution of Baltic Sea-derived pore water sulfate in the peatland soil based on major geochemical~~
80 ~~gradients delineated by brackish and freshwater tracers~~
81 - [track the fate of Baltic Sea-derived sulfate and](#) uncover potential S transformation pathways using concentration and
82 stable isotope measurements of pore water SO_4^{2-} ($\delta^{34}\text{S}$ and $\delta^{18}\text{O}$) and solid S compounds interpreted in the light of the
83 bacterial community structure and the presence of sulfate-reducing bacteria
84 - describe dissimilatory C decomposition pathways and methane cycling processes in relation to the found S
85 transformation patterns based on concentration and stable isotope measurements of CH_4 ($\delta^{13}\text{C}$, $\delta^2\text{H}$) and dissolved
86 inorganic C (DIC, $\delta^{13}\text{C}$) as well as to the abundance and community structure of methanogenic and methanotrophic
87 archaea

88 We hypothesized the marine legacy effect to express as lateral gradient in electrical conductivity (EC) and pore water sulfate
89 along the brackish-terrestrial transect. We further expected increasing terrestrial impact to promote the deprivation of the
90 brackish sulfate pool and to induce complementary patterns of methane production.

91 2. Material and Methods

92 2.1 Study site and sampling design

93 The study site is part of the nature reserve ‘Heiligensee und Hütelmoor’, a 490 ha coastal peatland complex located in NE
94 Germany directly at the SW Baltic coast with an elevation between -0.3 and + 0.7 m above sea level (Dahms, 1991) (latitude
95 $54^\circ 12'$, longitude $12^\circ 10'$, Fig. 1). Climate is transitional maritime with continental influence from the east. The area receives
96 a mean annual precipitation of 645 mm with a mean annual temperature of 9.2°C (reference period 1982-2011, data from the
97 German Weather Service (DWD)). Peat formation was initiated by the Littorina Sea transgression and the post-glacial sea
98 level rise around 5400 BC. Presently, the Hütelmoor is fed by a 15 km^2 forested catchment dominated by gley over fine sands.
99 Originally, the fen exhibited 0.2-2.3 m deep layers of sulfidic reed-sedge peat underlain by Late Weichselian sands over

impermeable till (Bohne & Bohne, 2008, Voigtländer *et al.*, 1996). Forty years of drainage for grassland use caused severe degradation of the peat, which was recently identified as sapric histosol (Koebsch *et al.*, 2013). Since the rewetting by flooding in 2010 through the construction of a weir at the outflow of the catchment, more than 80% of the area have been permanently inundated with freshwater from the surrounding forest catchment (Miegel *et al.*, 2016). Current vegetation of the Hütelmoor is dominated by patches of competitive emergent macrophytes such as reed and sedges (~~Common Reed~~ (*Phragmites australis* (Cav.) Trin. ex Steud and *Carex acutiformis* Ehrh.) that increasingly supersede species indicative for brackish conditions (*Bolboschoenus maritimus* (L.), *Palla Schoenoplectus tabernaemontani* (C. C. Gmel.) Palla) (Koch *et al.*, 2017). Under natural coastal dynamics, the Hütelmoor is episodically flooded by storm surges. Low outflow and high evapotranspiration rates promote brackish conditions. Major brackish water intrusions were reported for 1904, 1913, 1949, 1954 and 1995 (Bohne & Bohne, 2008) though flooding frequency is reduced since the site was dyked in 1903. Additional brackish input occurs through underground flow and atmospheric deposition as well as through high water situations at the Baltic Sea when backwater of the interconnected Warnow river delta enters the fen. However, potential brackish water entry paths other than storm surges have revealed negligible effect on peat salinity (Selle *et al.*, 2016). The last flooding event in 1995 raised EC in the drainage ditches up to 8 mS cm⁻¹, but the EC decreased to the pre-flooding level of 2 mS cm⁻¹ within the following five years (Bohne & Bohne, 2008). Samples were collected at four spots along a transect with increasing distance to the Baltic Sea (300-1,500m, Fig. 1b) within two weeks in October/November 2014. The transect included the area of a former study which revealed high concentrations of brackish SO₄²⁻ with annual means up to 23.7±3.2 mM (unpublished, Fig. 1c). At the time of sampling, water depth above peat surface spanned from 945 to 2519 cm, which presented the lowest range within the seasonal water level fluctuation. Sampling depth ranged from 45 to 65 cm which was in most cases sufficient to cover the full peat depth incl. the underlying mineral soil.

2.2 Pore water analysis

Pore waters were collected from distinct depth below the surface (cmbsf.) with a stainless steel push-point sampler attached to a syringe to draw the sample from a distinct penetration depth. Temperature, pH, EC and salinity were measured directly after sampling (Sentix 41 pH probe and a TetraCon 325 conductivity-measuring cell attached to a WTW multi 340i handheld; WTW, Weilheim). Samples were filtered (0.45 µm membrane syringe filters) in situ and transferred without headspace into vials (except for dissolved CH₄). Vials had been previously preconditioned with 1 M HCl and subsequent 1 M NaOH and were filled with a compound-specific preservative (see below). Dissolved CH₄ concentration was measured with the headspace approach. Therefore, 5 ml of pore water were transferred into 12 ml septum-capped glass vials under atmospheric pressure. Before taking them to the field, the sampling vials were flushed with Ar and filled with 500 µl saturated HgCl solution to prevent further biological activity. After sampling, the punctuated septum was covered with lab foil and the vials were stored upside down to minimize CH₄ loss. Headspace gas concentrations after equilibration were measured in duplicates with an Agilent 7890A gas chromatograph equipped with a flame ionization

Formatiert: Schriftart: Nicht Kursiv

133 detector and with a carbon plot capillary column or HP-Plot Q (Porapak-Q) column. Helium was used as tracer gas. Gas sample
134 analyses were performed after calibration of the gas chromatograph with standard gas that achieved reproducibility > 98.5%.
135 The measured headspace CH₄ concentration was then converted into dissolved CH₄ concentration using the temperature-
136 corrected solubility coefficient (Wilhelm *et al.*, 1977).
137 Samples for anion concentrations (SO₄²⁻, Cl⁻, Br⁻) were filled in 20 ml glas vials preserved with 1 ml 5% ZnAc-solution to
138 prevent sulfide oxidation. Anion concentrations were analyzed by IC (Thermo Scientific Dionex) in a continuous flow of 9
139 mM NaCO₃ eluent in an Ion Pac AS-9-HC 4 column, partly after dilution of the sample. The device was calibrated with NIST
140 SRM standard solutions freshly prepared before each run to span the concentration ranges of the (diluted) samples.
141 Reproducibility between sample replicates was better than ±5%.
142 For H₂S analysis, pore water was filled into 5 ml polypropylene vials and preserved with 0.25 ml 5% ZnAc solution. H₂S
143 concentration was measured photometrically (Specord 40, Analytic Jena) using the methylene blue method (Cline, 1969).
144 The metal and total dissolved S (TS_{diss}) concentrations were analysed by ICP-OES (iCAP 6300 DUO Thermo Fisher Scientific)
145 after appropriate dilution. Since high amounts of DOC may cause severe interferences in the ICP-OES element measurements,
146 samples were boiled in Teflon beakers with 65% HNO₃ and subsequent 19% HCl prior to analysis. The accuracy and precision
147 was routinely checked with the certified CASS standards as described previously (Kowalski *et al.*, 2012). The residual, non-
148 specified S fraction (ResS resulting from the difference between TS_{diss}, H₂S and SO₄²⁻ is suggest to consist primarily of
149 dissolved organic S, polysulfides, and S intermediates.
150 δ¹³C and δD values of methane were analyzed using the gas chromatography-combustion-technique (GC-C) and the gas
151 chromatography-high-temperature-conversion-technique (GC-HTC). The gas was directly injected in a Gas Chromatograph
152 Agilent 7890 (Agilent Technologies, Germany), the peaks were separated using a CP-PoraBOND Q GC-column
153 (50mx0.32mmx5µm, isotherm 60°C, Varian). Methane was quantitatively converted to the analysis gases CO₂ and H₂ in the
154 GC-Isolink-Interface (Thermo Finnigan, Germany) and directly transferred via open split interface (ConFlo IV, Thermo
155 Finnigan, Germany). The δ¹³C and δD values of both gases were then measured with the isotope-ratio-mass-spectrometer
156 MAT-253 (Thermo Finnigan, Germany). Results for δ¹³C ratios of methane are given in the usual δ-notation versus the Vienna
157 PeeDee Belemnite (VPDB) standard. δD-CH₄ ratios were referenced to the Vienna Standard Mean Ocean Water (V-SMOW).
158 The carbon isotope values (δ¹³C) of DIC were measured from a HgCl₂-preserved solution using a Thermo Finnigan MAT 253
159 gas mass spectrometer coupled to a Thermo Electron Gas Bench II via a Thermo Electron Conflo IV split interface. NBS19
160 and LSVEC were used to scale the isotope measurements to the VPDB standard. Based on replicate measurements of standards,
161 reproducibility was better than ±0.1‰ (Winde *et al.*, 2014). The stable carbon isotope ratio of DOC (δ¹³C) was determined
162 according to Ertl and Spitzzy (2004), involving cryogenic trapping of CO₂ and isotope ratio mass spectrometry with a Finnigan
163 Mat 252 with dual-inlet system. A modified combustion module was coupled on-line to the cryogenic trap: before trapping, a
164 20-ml sample was combusted by way of continuous injection (0.85 ml min⁻¹) in a helium stream into a self-assembled high
165 temperature catalytic oxidation unit, consisting of a furnace heated to 950 °C and a quartz glass column filled with copper
166 oxide and cerium oxide. Combustion gases were dried using Peltier-coolers and a magnesia perchlorate trap. ¹³C/¹²C-values

Formatiert: Tiefgestellt

Formatiert: Tiefgestellt

Formatiert: Tiefgestellt

Formatiert: Hochgestellt

(‰) were obtained from at least duplicate analyses and referenced to the VPDB standard. The standard deviation was smaller than 0.5‰.

For the determination of sulfate isotope signatures, dissolved sulfate was precipitated with 5% barium chloride as barium sulfate as described in Böttcher *et al.* (2007) (Böttcher *et al.*, 2007). After precipitation the solid was filtered, washed and dried, and further combusted in a Thermo Flash 2000 EA elemental analyzer that was connected to a Thermo Finnigan MAT 253 gas mass spectrometer via a Thermo Electron ConFlo IV split interface with a precision of better than ± 0.2 ‰. Isotope ratios are converted to the VCDT scale (Mann *et al.*, 2009) following Mann *et al.* (2009). For oxygen isotope analyses, BaSO₄ was decomposed by means of pyrolysis in silver cups using a high temperature conversion Elemental Analyzer (HTO-, Hekatech, Germany) connected to an isotope gas mass spectrometer (Thermo Finnigan MAT 253) (Kornexl *et al.*, 1999) at the Helmholtz Centre for Environmental Research—UFZ according to the method described by Kornexl *et al.* (1999). The calibration took place via the reference materials IAEA-SO-5 and -SO-6 and ¹⁸O/¹⁶O values were referenced to the V-SMOW standard. Replicate measurements agreed within ± 0.5 ‰.

Stable oxygen (O) isotope measurements of pore waters were conducted using a CRDS system (Picarro L2140-i) versus the V-SMOW standard. International V-SMOW, SLAP, and GISP, besides in-house standards were used to scale the isotope measurements. The δ -values are equivalent to milli Urey (mU) (Brand & Coplen, 2012) (Brand and Coplen 2012).

2.3 Sediment analysis

Intact peat cores were collected with a perspex liner (ID: 59.5 mm) and subsequently punched out layer-by-layer. The peat section protruding from the end of the liner was divided into 3 subsamples for the analysis of (i) Total reduced inorganic S (TRIS), (ii) total solid S (TS_{solid}) and reactive iron, and (iii) the microbial community structure. In order to minimize oxygen contamination, the outer layer of the peat core was omitted and subsamples were immediately packed. The aliquot for TRIS analysis was preserved with 1:1 (v/v) 20% ZnAc. Subsamples for microbial analysis were immediately stored in RNAlater to preserve DNA and RNA. A second core was taken for the analysis of water content and dry bulk density. TS_{solid} and TRIS samples were frozen within 8 hrs after collection. Aliquots for TS_{solid} elemental analysis were further freeze-dried and milled in a planet-ball mill.

TS contents were analyzed by means of dry combustion using an Eltra CS 2000 after combustion at 1250°C. The device was previously calibrated with a certified coal standard and precision is better than ± 0.02 %.

TRIS fractions were determined by a two-step sequential extraction of iron-monosulfides and pyrite (Fossing & Jørgensen, 1989). The acid volatile sulfur (AVS) fraction was extracted by the reaction with 1 M HCl for 1 h under a continuous stream of di-nitrogen gas. The H₂S released was quantitatively precipitated as ZnS and then determined spectrophotometrically with a Specord 40 spectrophotometer following the method of Cline (1969). The eChromium-reducible fraction-sulfur (CRS; essentially pyrite (FeS₂)), was extracted with hot acidic Cr(II)chloride solution. For δ^{34} S analysis in different TRIS fractions the ZnS was converted to Ag₂S by addition of 0.1 M AgNO₃ solution with subsequent filtration, washing and drying of the AgNO₃ precipitate as described by (Böttcher & Lepland, 2000). The non-specified solid S fraction, resulting from the

Formatiert: Tiefgestellt

200 difference between TS_{solid} , CRS and AVS, was suggested to present primarily organic-bond S (orgS). The $\delta^{34}S$ composition of
 201 this residual fraction was measured from the washed and dried solid residue after the Cr(II) extraction step via C-IRMMS
 202 following the approach of Passier (1999). The amount and stable isotope composition of organically bond sulfur was measured
 203 from the washed and dried solid residue after the Cr(II) extraction step via C-IRMMS following the approach of Passier (1999).
 204 Reactive iron was extracted from freeze-dried sediments by the reaction with a 1 M HCl solution for 1 h (e.g., Canfield, 1989).
 205 Iron was determined as Fe^{2+} after reduction with hydroxylamine hydrochloride via spectrophotometry using ferrozine as
 206 complexing agent following Stookey (1970). (Stookey, 1970). Reactive iron here is considered as the sum of those iron
 207 fractions that still may react with dissolved sulfide. The extracted iron fraction. This fraction consists includes of iron-(III)
 208 oxyhydroxides and iron-(II) monosulfides and acid volatile sulfide (AVS, essentially FeS) as well as a very minor contribution
 209 from dissolved Fe^{2+} in the pore water (Canfield, 1989). (Canfield, 1989).

210 2.4 Microbial community analysis

211 Genomic DNA of 0.2-0.3 g sediment was extracted with the EurX Soil DNA Kit (Roboklon, Berlin, Germany) according to
 212 manufactory protocols. DNA concentrations were quantified with a Nanophotometer® P360 (Implen GmbH, München, DE)
 213 and Qubit® 2.0 Fluorometer (Thermo Fisher Scientific, Darmstadt, Germany) according to the manufactory protocols.
 214 The 16S rRNA gene for bacteria was amplified with the primer combination S-D-Bact-0341-b-S-17 and S-D-Bact-0785-a-A-
 215 21 (Herlemann *et al.*, 2011). The 16S rRNA gene for archaea was amplified with the primer combination S-D-Arch-0349-a-
 216 S-17 and S-D-Arch-0786-a-A-20 (Takai & Horikoshi, 2000). The primers were labelled with unique combinations of
 217 barcodes. The PCR mix contained 1x PCR buffer ($Tris \cdot Cl$, KCl , $(NH_4)_2SO_4$, 15 mM $MgCl_2$; pH 8.7) (QIAGEN, Hilden,
 218 Germany), 0.5 μM of each primer (Biomers, Ulm, Germany), 0.2 mM of each deoxynucleoside (Thermo Fisher Scientific,
 219 Darmstadt, Germany) and 0.025 U μl^{-1} hot start polymerase (QIAGEN, Hilden, Germany). The thermocycler conditions were
 220 95°C for 5 minutes (denaturation), followed by 40 cycles of 95°C for 1 minute (denaturation), 56°C for 45 seconds (annealing)
 221 and 72°C for 1 minute and 30 seconds (elongation), concluded with a final elongation step at 72°C for 10 minutes. PCR
 222 products were purified with a Hi Yield® Gel/PCR DNA fragment extraction kit (Süd-Laborbedarf, Gauting, Germany)
 223 according to the manufactory protocol. PCR products of three individual runs per sample were combined. PCR products of
 224 different samples were pooled in equimolar concentrations and compressed to a final volume 10 μl with a concentration of
 225 200 ng μl^{-1} in a vacuum centrifuge Concentrator Plus (Eppendorf, Hamburg, Germany). Individual samples were sequenced
 226 in duplicates.
 227 The sequencing was performed on an Illumina MiSeq sequencer by the company GATC. The library was prepared with the
 228 MiSeq Reagent Kit V3 for 2x 300 bp paired-end reads according to the manufactory protocols. For better performance due to
 229 different sequencing length we used 15% PhiX control v3 library.
 230 The quality of the sequences was checked using the fastqc tool (FastQC A Quality Control tool for High Throughput Sequence
 231 Data; <http://www.bioinformatics.babraham.ac.uk/projects/fastqc/> by S. Andrews). Raw Ssequence—raw reads were
 232 demultiplexed, and barcodes were removed with the CutAdapt tool (Martin, 2011). The subsequent steps included merging of

Formatiert: Hochgestellt

reads using overlapping sequence regions (PEAR, Zhang et al. 2013), standardizing the nucleotide sequence orientation, and trimming and filtering of low quality sequences (Trimmomatic, ~~Bolger et al. 2014~~) (Bolger et al., 2014). After quality filtering, chimera were removed by the ChimeraSlayer tool of the QIIME pipeline. Subsequently, sequences were clustered into operational taxonomic units (OTU) at a nucleotide cutoff level of 97% similarity and singeltons were automatically deleted. To reduce noise in the dataset, sequences with relative abundances below 0.1% per sample were also removed. All archaeal libraries contained at least > 18,500 sequences, while bacterial libraries contained at least >12,500 sequences. OTUs were taxonomically assigned employing the GreenGenes database 13.05 (McDonald et al., 2012) using the QIIME pipeline (Caporaso et al., 2010). Representative sequences of OTUs were checked for correct taxonomical classification by phylogenetic tree calculations in the ARB environment. Relative abundance of sequences related to known methanogens, anaerobic methanotrophs (ANME) and sulfate reducers were used to project microbial depth profiles. Sequences have been deposited at NCBI under the Bioproject PRJNA356778 with the sequence read archive accession numbers SRR5118134-SRR5118155 for bacterial and SRR5119428-SRR5119449 for archaeal sequences, respectively.

3. Results

3.1 Pore water geochemical patterns and pore water isotope composition

Substantial amounts of dissolved salts with EC maxima of up to 11.5 mS cm⁻¹ occurred at peat depths below 30 cmbsf. (cm below surface, Fig. 2a, Table A1) and corresponded with brackish pore water proportions of up to 60% (based on Baltic Sea salinity reported by (Feistel et al., 2010). Only at spot 1, with the greatest distance to the coastline, lower EC values (max. 3.4 mS cm⁻¹) indicated minor brackish pore water proportions (5-6%). At the other three spots, EC values were similar, i. e., exhibited no lateral salinity graduation along the remaining Baltic Sea-freshwater transect. Vertical trends in pore water stable O isotope composition were similar for all spots and complementary to the salinity/EC patterns with an average upwards increase from 60 to 10 cmbsf. (Fig. 2b). The resulting salinity-δ¹⁸O relationship was negative (except for the low salinity gradient at freshwater spot 1) and thus inverse to the common salinity-δ¹⁸O trend characteristic for Baltic coastal waters (Fig. 2c). This suggests that distribution patterns of salinity have formed independently from evaporation effects confined to the top pore water layers. The pore water geochemistry in the peatland was increasingly diversified with depth: while the top 10 cmbsf. were comparatively homogenous across all spots, specific patterns evolving from diagenetic differences emerged primarily in deeper pore waters. Principal component analysis (Fig. 3) revealed the pore water geochemical composition below 10 cmbsf. to be constrained by two major components that evolved in opposed lateral directions and, in concert, explained 90% of the variation in pore water composition. A distinct gradient associated with a depth increase of EC and the associated conservative ions (Cl⁻, Na⁺, Br⁻) suggests a persistent brackish impact at spots 2, 3 and 4 (first principal component, explained 55% of the total variation). Only at spot 1, farthest away from the coastline, the EC increase with depth ~~was minute..~~ This EC gradient was

further negatively correlated with pH, indicating a general decrease in pH with depth and highest pH values around 7.0 at spot 1. A second distinct lateral gradient was delineated by the concentrations of dissolved Fe, Mn, DIC, and Ca which occurred in higher abundances at spot 1 and 2 closest to the upstream terrestrial catchment boundary (second principal component, explained 35% of the total variation). Such a lateral shift in pore water geochemistry is probably related to the supply of mineral solutes from terrestrial inflow. In this regard, the pore water composition of spot 2 unites the elevated supply in mineral compounds from terrestrial inflow with persisting remnants of former brackish impact.

3.2 Sulfur speciation, S isotope patterns and sulfate reducing communities

We found distinct differences in the S biogeochemical patterns across spots indicating different sulfate supply and transformation processes along the terrestrial-brackish continuum. In the following, we structured the results spot-wise according to the specific S regime and discuss first spot 1 (low solid sulfur and low sulfate), then spots 3 and 4 (high solid sulfur and low sulfate) and finally spot 2 (high solid sulfur and partially high sulfate concentrations).

3.2.1 Spot 1

Spot 1 characterized by low salinities and implied mineral inflow from the near freshwater catchment, exhibited the lowest sulfate concentrations of ≤ 0.3 mM, and H_2S concentrations were below detection limit hardly exceeded the detection limit (~ 1 μM , Fig. 4). Sulfate made up only a small proportion of the total dissolved S pool, thereby indicating a higher abundance of a non-specified dissolved S fraction, probably composed of dissolved organic S, polysulfides, and S intermediates.

In addition, the abundance of solid S was lowest at spot 1 (≤ 0.7 %dwt $\text{TS}_{\text{solid}}/\text{total S}$). Among solid S compounds, organic-bond S constituted the dominant solid S fraction (0.12 to 46.5 %dwt) with relatively stable $\delta^{34}\text{S}$ ratios (+8.1 and +9.8‰). Pyrite contents (measured as CRS) were low despite of abundant pore water Fe and available solid iron (Fig. 5). Only at spot 1, we found a low though consistent abundance of iron mono-sulfides (0.05-0.081 %dwt, measured as AVS). Biogeochemical turnover processes here might operate under sulfate-limited conditions resulting in lower sedimentary S contents and accumulation of iron monosulfides.

In correspondence with the low sulfate contents, no sulfate reducing bacteria occurred at spot 1.

3.2.2 Spots 3 and 4

Despite the persisting brackish impact found in the deeper pore waters of spots 3 and 4 closest to the Baltic Sea, we found only hardly any low abundances of pore water sulfate in the top 205 cmbsf. (0.3-0.5 \leq 0.1 mM), concentrations below detection limit (~ 0.001 mM) in a depth range of 10 to about 30 cmbsf., and only moderate SO_4^{2-} levels below down to 30 cmbsf. (0.1-1 mM). H_2S abundance was essentially restricted to depth at spot 3 (up to 3470.4 mM μM).

Low porewater sulfate concentrations prevented $\delta^{34}\text{S}$ measurements at the majority of the data points. However, the single $\delta^{34}\text{S}$ value of +86.4‰ measured at 60 cmbsf. of spot 3 (Fig. 6a) indicates a remarkable ^{34}S enrichment in relation to Baltic Sea water SO_4^{2-} (+21‰; Böttcher et al., 2007). Sulfur isotope fractionation to this extent is likely to result from a superposition of enzymatic kinetic fractionation associated with a reservoir effect and constitutes striking isotopic evidence for the exhaustion

Formatiert: Tiefgestellt

Formatiert: Tiefgestellt

of the brackish sulfate pool by intense DSR (Hartmann & Nielsen, 2012). Despite the missing isotopic evidence, it is likely, that the low sulfate concentrations at the remaining depth sections of spot 3 and along the depth profile of spot 4 result from the same intense sulfate reduction processes.

Correspondingly At the depths of potentially high DSR, we measured high amounts of total solid S (TS up to 3.54% dwt) at depth of spot 3. In both, spot 3 and 4, Organic-bond S constituted the dominant solid S fraction (0.25 to 1.63.3 % dwt) in these spots, but was completely missing at depth of spot 4. Pyrite was less abundant (0.2-0.3 % dwt) and exhibited a wide range of $\delta^{34}\text{S}$ ratios less abundant (max 0.3% dwt) and exhibited a wide range of $\delta^{34}\text{S}$ ratios ranging from (-15 to +11‰). As pyrite $\delta^{34}\text{S}$ ratios essentially reflect the isotopic signature of the microbially derived sulfide pool (Butler *et al.*, 2004, Price & Shieh, 1979), the found variation in pyrite $\delta^{34}\text{S}$ ratios reflected different stages of a differentiated reservoir effect that amplifies the enzymatic kinetic fractionation of DSR and varies in response to the openness of the system (i. e. connectivity to the sea).

In correspondence with the exhaustion of the brackish sulfate pool, the relative abundance of SRB was generally small (<5%) and most likely substrate-limited. SRB were from the *Deltaproteobacteria* class and the *Thermodesulfobionaceae* genus of the *Nitrospirae* phylum. With 40% relative abundance, *Chloroflexi* of the class *Dehalococcoidetes* represented the dominating bacterial group at the 1 mM SO_4^{2-} concentration depth of spot 3.

3.2.3 Spot 2

At spot 2 - the interface between brackish impact and mineral inflow from the freshwater catchment - we found a sharp rise in SO_4^{2-} concentration from ≤ 0.3 mM at the top 20 cm up to 32.833 mM at 60 cmbsf. The latter exceeded the quantities expected from marine supply (Feistel *et al.*, 2010, Kwiecinski, 1965) by a factor of 8. The pronounced concentration gradient at spot 2 was associated with a remarkable variation in the stable isotope composition showing a downcore decrease in $\delta^{34}\text{S}$ - SO_4^{2-} from +82.9 to +22.7‰ and a decrease in $\delta^{18}\text{O}$ - SO_4^{2-} from +30 to +11‰ (Fig. 6a). $\delta^{34}\text{S}$ values >+80‰ at 30 cmbsf. of spot 2 suggest the brackish sulfate pool in the top pore waters to be microbially exhausted under the same reservoir effect as in spots 3 and 4. The $\delta^{18}\text{O}$ and $\delta^{34}\text{S}$ ratios of excess SO_4^{2-} in 60 cmbsf. ($\delta^{34}\text{S}$: +22.7‰, $\delta^{18}\text{O}$: +11.4‰) corresponded well with modern day seawater SO_4^{2-} ($\delta^{34}\text{S}$: +21‰, $\delta^{18}\text{O}$: +9‰, Böttcher *et al.*, 2007). Altogether, the sharp sulfate concentration and isotope gradients at spot 2 could demonstrate the entire spectrum of sulfate speciation from the persistence of a marine sulfate reservoir at 60 cmbsf. towards progressing sulfate depletion in the upper peat layers.

To test this hypothesis, we applied a closed-system (Rayleigh-type) model (Eq. (1), Mariotti *et al.*, 1981) to the data from spot 2 and gained an estimate for the $\delta^{34}\text{S}$ ratios of the initial SO_4^{2-} reservoir ($\delta^{34}\text{S}_{\text{SO}_4^{2-}\text{initial}}$) and the kinetic isotope enrichment factor ϵ :

$$\delta^{34}\text{S}_{\text{SO}_4^{2-}\text{depth}} - \delta^{34}\text{S}_{\text{SO}_4^{2-}\text{initial}} = \epsilon \ln(f\text{SO}_4^{2-}\text{depth}) \quad (1)$$

Here $\delta^{34}\text{S}_{\text{SO}_4^{2-}\text{depth}}$ represents the S isotope values measured in specific depths of spot 2, and $f\text{SO}_4^{2-}\text{depth}$ constitutes the fraction of remaining pore water SO_4^{2-} in relation to the initial sulfate reservoir (32.83 mM SO_4^{2-} , measured in 60 cmbsf at spot 2). The fit through four data points (R^2 : 0.99; $p > 0.05$) revealed the $\delta^{34}\text{S}$ ratios of the initial SO_4^{2-} reservoir (+24‰) to be close to the

³⁴S signature of the Baltic Sea (Fig. 6b). The isotopic offset is within the uncertainty of the estimate. The isotope enrichment factor ϵ was estimated to be -27‰ which is within the range reported for DSR in laboratory studies with pure cultures (Canfield, 2001, Kaplan & Rittenberg, 1964, Sim *et al.*, 2011) and in the field (Böttcher *et al.*, 1998, Habicht & Canfield, 1997). The pronounced sulfate distribution patterns at spot 2 went along with the highest amounts of pyrite (0.458-1.436 %dwt.). Pyrite contents increased with depth and partially -that exceeded the amounts of organic-bond S_ (0.38-1.26 %dwt.). The patterns in pyrite $\delta^{34}\text{S}$ ratios did not correspond with the vertical trend in sulfate availability. Instead $\delta^{34}\text{S}$ values were lowest in 20 cmbsf. (-15‰) and stabilized around +2‰ below. Interestingly, at peak sulfate supply of spot 2, the relative abundance of *Deltaproteobacteria* did not exceed 5%. Instead, the SRB community at depth was dominated by the *Thermodesulfobionaceae* genus that contributed up to 21% of all bacterial 16S rRNA sequences. Likewise with spot 3, *Chloroflexi* of the class *Dehalococcoidetes* represented also the dominating bacterial group at depth of spot 2.

3.3 Dissolved methane concentrations, isotopic signature and methanogenic communities

Measured pore water CH₄ concentrations were up to 0.7 mM/643 μM with equivocal vertical patterns across spots (Fig. 7a), reflecting the methane-specific spatial variability that evolves from small-scale heterogeneity in production and consumption processes and from ebullitive release events (Chanton *et al.*, 1989, Whalen, 2005). Here, we use the isotope composition of CH₄ (Fig. 7b) and DIC (Fig. 7c) to provide a clearer (and probably more robust) indication for patterns of methanogenesis and methanotrophy. Methanogenesis is a highly fractionating process: in comparison to the starting organic material ($\delta^{13}\text{C}$ ~-27‰ in this study), the produced CH₄ is distinctively ¹³C-depleted, whilst at the same time, CO₂ becomes considerably enriched in ¹³C (Whiticar *et al.*, 1986)(Whiticar *et al.*, 1986). The isotope composition of CH₄ (Fig. 7b) and DIC (Fig. 7c) provided a clearer (and probably more robust) indication for patterns of methanogenesis and methanotrophy. With this respect, High $\delta^{13}\text{C}$ -DIC ratios up to +4.2‰ suggest intense methanogenic (i. e. ¹³C-DIC fractionating) processes in 20-40 cmbsf, whereas DIC on top was comparatively depleted in ¹³C as characteristic for methane oxidation in the aerated surface layers. $\delta^{13}\text{C}$ -DIC ratios below 40 cmbsf. converged towards the isotopic signature of bulk organic C (-26‰). At spot 2, we found the most pronounced downward drop in $\delta^{13}\text{C}$ -DIC ratios with a minimum of -23.9‰ in 60 cmbsf. This pattern coincided with a consistent downward decrease in $\delta^{13}\text{C}$ -CH₄ ratios from -57 to -68‰ and suggests that methanogenesis operates under higher ¹³C fractionation associated with thermodynamically less favorable conditions at the bottom of spot 2. δD ratios of methane did not exhibit a concurrent increase but varied unrelated to $\delta^{13}\text{C}$ -CH₄ ratios in a range between -333 and -275‰. Based on the C and D isotopic ratio threshold raised by Whiticar (1986), acetate fermentation revealed to be the dominant methane production pathway in our study site (Fig. 8). A concurrent rise in both δD - and $\delta^{13}\text{C}$ -CH₄ ratios at depth of spot 1 suggests a shift towards dominating CO₂ reduction and/or an increase in methanotrophy. Together with high $\delta^{13}\text{C}$ -DIC ratios in the upper parts of the peat, 16S rRNA sequences related to methanogens (Fig. 7d) provided further evidence for intensive methane production. At spot 2, we found the largest divergence with 90% methanogen-related sequences at the surface while in deeper regions (10-50 cmbsf.) less than 7% of the archaeal domain could be attributed

Formatiert: Hochgestellt

Formatiert: Tiefgestellt

Formatiert: Hochgestellt

Formatiert: Tiefgestellt

Formatiert: Hochgestellt

to methanogens. Surprisingly, at 60 cmbsf. of spot 2, methanogen percentages increased abruptly up to 41% despite of high relative abundances of SRB. Spot 1 exhibited the lowest methanogen proportions, that decreased from 21% at the top down to 1% in 50 cmbsf.

The methanogen community was mostly dominated by *Methanosaeta*, an obligate acetotrophic archaea genus that thrives in terrestrial organic-rich environments. *Methanosaeta* proportion usually scaled with the methanogen percentage, and contributed 70-100% to the methanogenic community.

The elucidation of in situ methanogenic pathways from the isotopic composition of CH₄ can be blurred by overlapping fractionation factors or the isotope effect of methanotrophy. However, the phylogenetic structure of the methanogenic community provided unequivocal evidence for acetate fermentation as the prevailing methanogenic pathway in most of the peatland.

Sequences related to aerobic methanotrophs of the genus *Methylosinus* were only found at 30 cmbsf. in spot 4 representing approximately 1.5% of all bacterial sequences (data not shown). Aerobic methanotrophs were underrepresented in our dataset.

Consistent with the concurrent depth increase in $\delta^{13}\text{C}\text{-CH}_4$ and $\delta\text{D}\text{-CH}_4$, spot 1 (Fig. 8), situated at the fringe of the freshwater catchment, exhibited high abundances of anaerobic methanotrophs of the ANME-2d clade, that are so far implicated to use NO₃⁻ (Raghoebarsing *et al.*, 2006) and/or Fe(III) (Ettwig *et al.*, 2016) as electron acceptor.

4. Discussion

4.1 Pore water biogeochemical patterns

Overall, the pore water geochemistry of the Hütelmoor is characterized by ~~lateral~~-legacy effects preserved ~~in-below~~ 20 to 30 cm depth that reflect the ~~lateral~~ brackish/terrestrial continuum and an overlying recent layer representing the prevalent freshwater regime induced by rewetting.

Despite a continuous ground water inflow from the forested catchment (Miegel *et al.*, 2016), relics of former brackish and mineral terrestrial inflow are preserved in the deeper layers of the relatively shallow peat body. This is exemplified by high pore water EC values that exceeded those reported directly after the last brackish water intrusion event in 1995 (Bohne & Bohne, 2008). In fact, discharge within the peatland is channeled through rapid flow in the drainage ditches while water movement within the interstitial peat body seems to be mostly restricted to vertical exchange processes (evaporation, precipitation) with minor lateral flow (Selle *et al.*, 2016). Therefore, we assume that drainage-induced hydrological alterations reinforce the segregation of the peat pore matrix from subsurface lateral exchange. This allows for the preservation of residual signals in deeper pore waters and confines contemporary biogeochemical transformation processes to the recycling of autochthonous matter. ~~The new top freshwater layer which established after flooding in 2010, overprinted lateral differences along the brackish/fresh continuum and now shapes the upper pore water geochemistry in the entire peatland.~~
~~The newly top freshwater layer that established freshwater layer on top after flooding in 2010, overprints lateral differences along the brackish/fresh continuum and determines shapes the upper pore water geochemistry in the entire peatland.~~

394 4.2 Sulfur transformation

395 Along the entire brackish/terrestrial transect, virtually no sulfate was abundant in the newly developed fresh pore water layer
396 at the top 20 cm. However, distinct differences in sulfur speciation across spots were preserved below 20 cmbsf. and seemed
397 to reflect the gradual exposure to former brackish intrusion and terrestrial inflow.

398 Spot 1 appeared to be virtually un-affected by any brackish impact with biogeochemical turnover processes operating under
399 sulfate-limited conditions. Low sedimentary S contents and the accumulation of iron monosulfides as representative for
400 freshwater environments are strong points for this conclusion.

401 Also at spots 3 and 4, contemporary biogeochemical processes essentially operated under sulfate-limited conditions although
402 these areas had been exposed to flooding from the nearby Baltic Sea. High sedimentary S concentrations in conjunction with
403 the ^{34}S composition of the remaining sulfate suggest that the brackish sulfate reservoir has been essentially exhausted through
404 DSR with the produced sulfide being either incorporated as diagenetically derived S in organic compounds or precipitated as
405 ^{34}S -enriched pyrite minerals (Brown & MacQueen, 1985, Hartmann & Nielsen, 2012). Hence, if dyking of coastal wetlands
406 prevents the replenishment of the brackish sulfate reservoir, the latter can be almost completely consumed through DSR as has
407 been demonstrated by the Rayleigh distillation model. The rapid exhaustion of the brackish sulfate reservoir is likely to be
408 reinforced in coastal peatlands where vast amounts of C compounds constitute an extensive electron donor supply for DSR.

409 Prevalent sulfate-limitation at spots 1, 3 and 4 was reflected by the virtual absence of the sulfate reducing microbial community.
410 Interestingly, minor remnants of the brackish sulfate pool (1 mM SO_4^{2-}) at depth of spot 3 were associated with 40% relative
411 abundance of *Chloroflexi* of the class *Dehalococcoidetes*. Genomes of this group in marine sediments have been shown to
412 code for *dsrAB* genes (Wasmund *et al.*, 2016). Through their ability to reduce sulfite they may be involved in S redox cycling.
413 Indeed, further research is required to better establish their function in the S cycle.

414 S geochemistry at spot 2, which unites the effects of brackish water intrusion with mineral inflow of terrestrial origin, differed
415 substantially from the other spots with remarkably high sulfate concentrations (33mM) at depth. The mineral impact from
416 terrestrial inflow was not only reflected by high concentrations of dissolved constituents (Fe, DIC, Mg, Ca, Mn) but also by
417 high contents of labile iron minerals and dissolved ferrous iron. Interactions with poorly-ordered ferric hydroxides can supply
418 Fe(III) as competitive electron acceptor next to sulfate (Postma & Jakobsen, 1996) and may, therefore, inhibit the efficient
419 microbial reduction of the brackish sulfate reservoir. Amorphous ferric hydroxides effectively suppressed DSR in a recently
420 rewetted Baltic coastal wetland (Virtanen *et al.*, 2014). In our study, high contents of labile iron minerals and dissolved ferrous
421 iron at depth of spot 2, coincided with a high abundance of *Thermodesulfobivibrionaceae* at concurrently minor occurrence of
422 *Deltaproteobacteria*. Recent in vitro experiments suggest *Thermodesulfobivibrionaceae* can utilize ferric iron as electron
423 acceptor next to sulfate (Fortney *et al.*, 2016). Indeed, the demonstration of Fe(III) reduction by *Thermodesulfobivibrionaceae*
424 under in situ conditions is currently still pending. ~~But~~ Nevertheless, high contents of labile iron minerals, the remarkable
425 accumulation of pore water iron, and the absence of typical iron reducers (*Geobacteraceae*, *Peptococcaceae*, *Shewanellaceae*,
426 *Desulfobivibrionaceae*, *Pelobacteraceae*) could suggest *Thermodesulfobivibrionaceae* to prefer Fe(III) as electron acceptor over

Formatiert: Schriftart: Kursiv

sulfate. ~~Thus, the~~ unique SO_4^{2-} concentration patterns at spot 2 may ~~, thus,~~ be attributed to the inhibited microbial consumption of the brackish sulfate reservoir caused by the delivery of alternative electron acceptors from the nearby freshwater catchment. Altogether, our results demonstrate the fate of the brackish sulfate reservoir in coastal wetlands under closed system conditions caused by dyking. Microbial transformation processes have decoupled the sulfate distribution patterns from the relic brackish impact ~~delineated through conservative tracer ions~~ and have caused marked differences in contemporary sulfate biogeochemistry: ~~On the one hand, DSR exhausted the brackish sulfate reservoir in wide parts of the peatlands. On one hand, the brackish sulfate reservoir was efficiently exhausted by DSR,~~ whereas on the other hand, the preferential consumption of competitive electron acceptors from terrestrial origin allowed for the local accumulation of large sulfate concentrations. Indeed, these relic signals of brackish-terrestrial intermixing are constrained to the deeper pore water regions below 30 cmbsf. as recent rewetting measures established a homogeneous freshwater regime in the top layers of the entire peatland.

4.3 Methane production and consumption

$\delta^{13}\text{C}$ -DIC ratios and a thriving methanogenic community indicate the establishment of distinct methane production zones in the recently formed freshwater layer across the entire peatland. Interestingly, the methanogen community was dominated by *Methanosaeta*, an obligate acetotrophic genus of archaea typical of terrestrial organic-rich environments, indicating the prevalent freshwater characteristics of the newly formed pore water layer. Indeed, thermodynamically favorable methanogenic conditions were confined to the top layers since isotopic evidence and archaeal distribution patterns indicate a downward shift towards non-fractionating metabolic processes (Barker, 1936, Lapham *et al.*, 1999) at the bottom. This vertical transition was most pronounced at spot 2, probably indicating a potential suppression of methanogenesis by high concentrations of sulfate and labile ferric iron compounds at depth.

Surprisingly, we observed mutual coexistence of SRB (22% of all bacterial sequences) and methanogens (>40% of all archaeal sequences) at high SO_4^{2-} -concentrations (32.8 mM) in 60 cmbsf. at spot 2. Simultaneous methanogenesis and DSR have been reported under the abundance of methanol, trimethylamine or methionine as methanogenic precursors (Oremland & Polcin, 1982). However, the concurrent high abundance of *Methanosaeta* (30%) at depth of spot 2 suggests competitive consumption of acetate by both SRB and methanogens. Although Liebner *et al.* (2015) emphasized the relevance of community structure with regards to prevailing methanogenic pathways, total abundance data could potentially yield more insights to this issue.

Sequences related to aerobic methanotrophs of the genus *Methylosinus* were only found at 30 cmbsf. in spot 4 representing approximately 1.5% of all bacterial sequences (data not shown). The phenomenon of a lagged re/establishment of methanotrophs in comparison to methanogens after rewetting in this particular peatland is addressed in another publication (Wen *et al.*, 2018).

Despite the overlap of ~~modeled~~ methane production ~~zones anticipated from $\delta^{13}\text{C}$ -DIC ratios and with~~ sulfate reduction zones, we couldn't find evidence for the syntrophic consortium of anaerobic methanotrophs (ANME) and sulfate reducers that is commonly associated with ~~the anaerobic oxidation of methane coupled to sulfate reduction (AOM-SR)~~ AOM-SR in marine environments (Boetius *et al.*, 2000). However, we cannot exclude that AOM-SR is driven by archaea that are so far not known

Formatiert: Hochgestellt

for this function. One potential candidate phylum is the *Bathyarchaeota* that have been shown to encode an untypical version of the functional gene for methane production and consumption (methyl co-enzyme M reductase subunit A, *mcrA*) (Evans *et al.*, 2015). These archaea dominated spot 2 with 48-97% relative sequence abundance of the archaeal community between 10 and 60 cm (data not shown).

While we cannot supply microbial evidence for AOM-SR, high abundances of anaerobic methanotrophs of the ANME-2d clade at spot 1 suggest anaerobic methane oxidation coupled to electron acceptors of terrestrial origin. Methanotrophs of the ANME-2d clade are so far known to utilize NO_3^- (Raghoebarsing *et al.*, 2006) and ferric iron (Ettwig *et al.*, 2016) as electron acceptors, both of which were abundant at the respective spot. This observation is further supported by the trend in $\delta^{13}\text{C}\text{-CH}_4$ and $\delta\text{D}\text{-CH}_4$ ~~which-that~~ potentially indicates a downward increase in methanotrophy at spot 1. The biogeochemical characteristics at this very location result most likely from formerly drier conditions due to slightly higher elevation in combination with prevalent inflow from the nearby forest catchment.

Our results demonstrate how rewetting of a coastal peatland established a distinct freshwater regime in the upper pore water layers, which, in conjunction with prevalent anaerobic conditions and a vast stock of labile C compounds, offers favorable conditions for intense methane production and explains the high methane emissions reported in (Hahn *et al.*, 2015) and Koebisch *et al.* (2015). As intense methane production was confined to the upper pore water layers in the entire peatland, it did not interfere with high sulfate concentrations locally preserved as legacy of former brackish impact in the bottom. Instead, isotopic and microbial evidence suggested mineral compounds of terrestrial origin to constitute an electron acceptor for anaerobic methane oxidation, which is an often neglected - though important process in freshwater environments (Segarra *et al.*, 2015). Our results indicate that this process ~~occurs-can occur~~ also in disturbed coastal peatlands. Indeed, the quantitative effects of anaerobic methane consumption on methane emissions in coastal and/or rewetted peatlands need to be addressed in future studies.

5. Conclusions

In this study, we investigated the biogeochemical and hydrological mechanisms that turn disturbed and remediated coastal peatlands into strong methane sources. Our study demonstrates how human intervention overrides the sulfate-related processes that suppress methane production and thereby suspends the natural mechanisms that mitigate greenhouse gas emissions from coastal environments. Our study highlights how human intervention overrides the sulfate-related methane emission suppression processes that constitute a natural greenhouse gas mitigation mechanism in coastal environments. Hence, the climate effect of disturbed and remediated coastal wetlands cannot simply be derived by analogy with their natural counterparts. Instead, human alterations form new transient systems where relic brackish signals intermingle with recent freshwater impacts. The evolving biogeochemical patterns overprint naturally established gradients formed, for instance, by the distance to the coastline. In particular, the decoupling of sulfate abundance from salinity is of high practical relevance for greenhouse gas inventories that establish methane emission factors based on the empirical relation to salinity as easily accessible proxy for sulfate concentrations.

493 Coastal environments are subject to particular pressure by high population density while at the same time their potential as
494 coastal buffer zones is moving more and more into the focus of policy makers and land managers. From a greenhouse gas
495 perspective, the exposure of [embanked-dyked](#) wetlands to natural coastal dynamics would literally open the floodgates for a
496 replenishment of the marine sulfate pool and constitute an efficient measure to reduce methane emissions. However, in
497 practice, this option has to be weighed against concurrent land use aspects.

498 **6. Data availability**

499 Geochemical data are represented within this manuscript in the appendix (Table A1). Sequences have been deposited at NCBI
500 under the Bioproject PRJNA356778 with the sequence read archive accession numbers SRR5118134-SRR5118155 for
501 bacterial and SRR5119428-SRR5119449 for archaeal sequences, respectively.

7. Appendices

Table A1 Site parameters, pore water and soil characteristics. Water level and soil depth are given in cm above and cm below surface (cmasf. and cmbsf, respectively) Molar concentrations and dry weight ratios of dissolved and solid species

| Station | Water level cmasf. | Depth cmbsf | pH | Sal ppt | EC mS cm ⁻¹ | Cl ⁻ mM | Br ⁻ μM | Na ⁺ mM | TS _{diss} mM | SO ₄ ²⁻ mM | H ₂ S μM | TS _{solid} %dwt | CRS %dwt | AVS %dwt | orgS %dwt | CH ₄ μM | DIC mM |
|---------|-----------------------|----------------|-----|------------|---------------------------|-----------------------|-----------------------|-----------------------|--------------------------|-------------------------------------|------------------------|-----------------------------|-------------|-------------|--------------|-----------------------|-----------|
| 1 | 14 | 0 | 6.7 | 0.7 | 1.8 | 11.5 | 19.9 | 9.6 | 0.1 | 0.0 | 1 | 0.3 | 0.1 | 0.1 | 0.12 | 144 | 5.4 |
| | | 5 | 7.0 | 0.7 | 1.8 | 12.6 | 19.9 | 10.7 | 0.1 | 0.0 | 0 | 0.3 | 0.1 | 0.1 | 0.12 | 312 | 6.2 |
| | | 10 | 7.0 | 1.0 | 2.4 | 14.6 | 19.1 | 10.7 | 0.2 | 0.0 | 3 | 0.3 | 0.1 | 0.1 | 0.31 | 234 | 7.5 |
| | | 20 | 7.1 | 1.4 | 2.9 | 11.0 | 25.6 | 10.5 | 0.2 | 0.0 | 1 | 0.3 | 0.1 | 0.1 | 0.51 | 109 | 21.7 |
| | | 30 | 7.1 | 1.6 | 3.4 | 12.5 | 31.9 | 14.1 | 0.3 | 0.1 | 1 | 0.3 | 0.1 | 0.0 | 0.51 | 143 | 25.3 |
| | | 40 | 7.2 | 1.7 | 3.4 | 11.4 | 31.3 | 13.7 | 0.3 | 0.0 | 2 | 0.5 | 0.1 | 0.1 | 0.43 | 178 | 26.7 |
| | | 50 | 7.1 | 1.5 | 3.2 | 12.0 | 38.1 | 13.5 | 0.5 | 0.3 | 0 | 0.7 | 0.1 | 0.1 | 0.35 | 101 | 21.8 |
| 2 | 9 | 0 | 6.9 | 1.4 | 3.0 | 19.3 | 37.0 | 18.2 | 0.2 | 0.0 | 0 | 1.3 | 0.5 | 0.1 | 0.75 | 462 | 8.9 |
| | | 5 | 6.7 | 1.2 | 2.6 | 23.3 | 39.0 | 17.8 | 0.2 | 0.0 | 1 | 1.8 | 0.5 | 0.1 | 1.20.8 | 344 | 8.4 |
| | | 10 | 7.2 | 3.0 | 5.7 | 37.9 | 46.5 | 32.6 | 1.0 | 0.0 | 6 | 2.3 | 0.5 | 0.0 | 1.81.0 | 56 | 17.3 |
| | | 20 | 7.0 | 4.0 | 7.3 | 48.3 | 82.1 | 41.4 | 1.2 | 0.3 | 7 | 2.3 | 0.7 | 0.0 | 1.61.3 | 82 | 20.8 |
| | | 30 | 6.5 | 5.4 | 9.7 | 63.7 | 99.8 | 56.5 | 4.5 | 3.74 | 5 | 3.4 | 0.8 | 0.0 | 2.61.2 | 643 | 28.8 |
| | | 40 | 6.4 | 5.4 | 9.7 | 64.9 | 125.3 | 64.3 | 198.6 | 17.1 | 34 | 1.7 | 1.0 | 0.0 | 0.71.1 | 197 | 15.5 |
| | | 50 | 6.0 | 5.5 | 9.9 | 67.8 | 129.5 | 61.7 | 18.3 | 19.1 | 61 | 4.0 | 1.2 | 0.0 | 2.80.9 | 128 | 17.1 |
| 3 | 9 | 60 | 5.1 | 6.5 | 11.5 | 75.5 | 85.8 | 63.9 | 32.63 | 32.83 | 274 | 0.5 | 1.4 | 0.0 | 0.04 | 139 | 12.8 |
| | | 0 | 6.6 | 1.4 | 2.9 | 22.2 | 151.6 | 19.6 | 0.2 | 0.0 | 0 | 0.9 | 0.2 | 0.0 | 0.73 | 231 | 4.4 |
| | | 5 | 6.6 | 1.4 | 3.0 | 22.4 | 49.8 | 20.9 | 0.2 | 0.0 | 1 | 1.1 | 0.2 | 0.0 | 0.93 | 193 | 4.9 |
| | | 10 | 6.4 | 1.9 | 3.8 | 28.6 | 50.9 | 28.1 | 0.3 | 0.0 | 21 | 1.3 | 0.2 | 0.0 | 1.10.3 | 486 | 6.1 |
| | | 20 | 6.1 | 3.7 | 6.8 | 54.5 | 64.9 | 48.3 | 1.3 | 0.0 | 53 | 1.2 | 0.2 | 0.0 | 1.00.2 | 420 | 5.7 |
| | | 30 | 6.5 | 4.7 | 8.6 | 69.4 | 122.9 | 58.7 | 1.0 | 0.0 | 38 | 1.6 | 0.2 | 0.0 | 1.40 | 81 | 4.1 |
| | | 40 | 5.6 | 5.4 | 9.6 | 87.2 | 156.3 | 55.7 | 0.5 | 0.0 | 25 | 2.4 | 0.2 | 0.0 | 2.21.6 | 122 | 4.1 |
| 4 | 19 | 50 | 5.8 | 5.7 | 10.2 | 92.8 | 168.5 | 77.0 | 0.61 | 0.1 | 187 | 2.9 | 0.2 | 0.0 | 2.71.0 | 13 | 3.6 |
| | | 60 | 6.0 | 5.2 | 9.4 | 77.6 | 181.6 | 70.9 | 1.52 | 1.0 | 347 | 3.5 | 0.2 | 0.0 | 3.31.0 | 89 | 6.3 |
| | | 0 | 6.6 | 1.4 | 2.9 | 20.5 | 159.4 | 19.2 | 0.2 | 0.0 | 1 | 1.3 | 0.3 | 0.0 | 0.96 | 254 | 4.2 |
| | | 5 | 6.7 | 1.2 | 2.7 | 22.6 | 49.4 | 19.8 | 0.2 | 0.1 | 0 | 1.0 | 0.2 | 0.0 | 0.76 | 127 | 4.0 |
| | | 10 | 6.6 | 2.7 | 5.2 | 37.7 | 48.4 | 33.1 | 1.0 | 0.0 | 7 | 0.7 | 0.2 | 0.0 | 0.56 | 48 | 8.6 |
| | | 20 | 7.2 | 3.2 | 6.1 | 52.3 | 84.9 | 44.3 | 1.0 | 0.0 | 5 | 0.8 | 0.2 | 0.0 | 0.74 | 49 | 6.6 |
| | | 30 | 6.6 | 4.5 | 8.1 | 69.4 | 99.3 | 55.2 | 1.0 | 0.74 | 2 | 1.5 | 0.2 | 0.0 | 1.40.3 | 292 | 11.6 |
| | | 40 | 6.4 | 4.5 | 8.2 | 73.5 | 126.1 | 50.4 | 0.5 | 0.1 | 33 | 0.2 | 0.2 | 0.0 | 0.40.0 | 430 | 11.3 |

Formatiert: Hochgestellt

Formatiert: Hochgestellt

Formatiert: Hochgestellt

Formatiert: Tiefgestellt

Formatiert: Tiefgestellt

Formatiert: Zentriert

Formatiert: Zentriert

Formatiert: Zentriert

Formatiert: Zentriert

Formatiert: Zentriert

8. Author contributions

FK and MB have formulated the research question and planned the study design. FK acquired funding. FK, GJ, MK, MW and SK collected the samples. MB, SL, AS, MG, TS and SK provided resources and lab instrumentation for sample analysis. FK, AS, IS, MK, GJ, SK and JW conducted the geochemical analyses. MW, SL and VU conducted the microbial sequencing analysis. BL validated the results. FK visualized the data and prepared the original draft with contributions from all coauthors.

9. Competing interests

The authors declare that they have no conflict of interest

10. Acknowledgements

This work was supported by the DFG Research Training Group *BALTIC TRANSCOAST* (grant DFG GRK 2000) and the Helmholtz *Terrestrial Environmental Observatories (TERENO)* Network. This is *BALTIC TRANSCOAST* publication number GRK2000/023. FK was supported by the Helmholtz Association of German Research Centers through the Helmholtz Postdoc Programme (grant PD-129), the Helmholtz Climate Initiative *REKLIM* (Regional Climate Change). FK was further supported by the European Social Fund (ESF) and the Ministry of Education, Science and Culture of Mecklenburg-Western Pomerania within the scope of the project WETSCAPES (ESF/14-BM-A55-0030/16). TS and SL are each supported by a Helmholtz Young Investigators Group (grant VH-NG-821 and VH-NG-919). Biogeochemical and stable isotope work was supported by the Leibniz Institute for Baltic Sea Research (IOW). We wish to express our gratitude to L. Kretzschmann, A. Saborowski, and S. Strunk for their commitment to field work under tough conditions. B. Juhls and S. Strunk have helped with map creation. The study would not have been possible without the laboratory and bioinformatics support by A. Gottsche, A. Saborowski, L. Kretzschmann, A. Köhler, B. Plessen, V. Winde, U. Günther, F. Horn, X. Wen, and H. Baschek.

11. References

Barker HA (1936) On the biochemistry of the methane fermentation. *Archiv für Mikrobiologie*, 7, 404-419.

Boetius A, Ravenschlag K, Schubert CJ et al. (2000) A marine microbial consortium apparently mediating anaerobic oxidation of methane. *Nature*, 407, 623.

Bohne B, Bohne K (2008) Monitoring zum Wasserhaushalt einer auf litoralem Versumpfungsmoor gewachsenen Regenmoorkalotte—Beispiel Naturschutzgebiet „Hütelmoor“ bei Rostock. *Aspekte der Geoökologie*. Berlin: Weißensee Verlag.

Bolger AM, Lohse M, Usadel B (2014) Trimmomatic: a flexible trimmer for Illumina sequence data. *Bioinformatics*, 30, 2114-2120.

Böttcher M, Brumsack H-J, Dürselen C-D (2007) The isotopic composition of modern seawater sulfate: I. Coastal waters with
 535 special regard to the North Sea. *Journal of Marine Systems*, 67, 73-82.

Böttcher ME, Brumsack H-J, De Lange GJ, Robertson A (1998) Sulfate reduction and related stable isotope (^{34}S , ^{18}O)
 variations in interstitial waters from the Eastern Mediterranean. In: *Proceedings of the Ocean Drilling Program. Scientific
 Results*. pp 365-376. National Science Foundation.

Böttcher ME, Lepland A (2000) Biogeochemistry of sulfur in a sediment core from the west-central Baltic Sea: evidence from
 540 stable isotopes and pyrite textures. *Journal of Marine Systems*, 25, 299-312.

Brand WA, Coplen TB (2012) Stable isotope deltas: tiny, yet robust signatures in nature. *Isotopes in environmental and health
 studies*, 48, 393-409.

Brown K, Macqueen J (1985) Sulphate uptake from surface water by peat. *Soil Biology and Biochemistry*, 17, 411-420.

Butler IB, Böttcher ME, Rickard D, Oldroyd A (2004) Sulfur isotope partitioning during experimental formation of pyrite via
 545 the polysulfide and hydrogen sulfide pathways: implications for the interpretation of sedimentary and hydrothermal pyrite
 isotope records. *Earth and Planetary Science Letters*, 228, 495-509.

Canfield DE (1989) Reactive iron in marine sediments. *Geochimica et Cosmochimica Acta*, 53, 619-632.

Canfield DE (2001) Isotope fractionation by natural populations of sulfate-reducing bacteria. *Geochimica et Cosmochimica
 Acta*, 65, 1117-1124.

550 Caporaso JG, Kuczynski J, Stombaugh J et al. (2010) QIIME allows analysis of high-throughput community sequencing data.
Nature methods, 7, 335.

Chanton JP, Martens CS, Kelley CA (1989) Gas transport from methane-saturated, tidal freshwater and wetland sediments.
Limnology and Oceanography, 34, 807-819.

Cline JD (1969) Spectrophotometric determination of hydrogen sulfide in natural waters 1. *Limnology and Oceanography*, 14,
 555 454-458.

Dahms P (1991) Studie Wasserregulierung Hütelmoor. Universität Rostock, Fachbereich Landeskultur und Umweltschutz,
 Fachgebiet Kulturtechnik.

Deverel SJ, Ingrum T, Leighton D (2016) Present-day oxidative subsidence of organic soils and mitigation in the Sacramento-
 San Joaquin Delta, California, USA. *Hydrogeology journal*, 24, 569-586.

560 Deverel SJ, Rojstaczer S (1996) Subsidence of agricultural lands in the Sacramento-San Joaquin Delta, California: Role of
 aqueous and gaseous carbon fluxes. *Water Resources Research*, 32, 2359-2367.

Erkens G, Van Der Meulen MJ, Middelkoop H (2016) Double trouble: subsidence and CO₂ respiration due to 1,000 years of
 Dutch coastal peatlands cultivation. *Hydrogeology journal*, 24, 551-568.

Ettwig KF, Zhu B, Speth D, Keltjens JT, Jetten MS, Kartal B (2016) Archaea catalyze iron-dependent anaerobic oxidation of
 565 methane. *Proceedings of the National Academy of Sciences*, 113, 12792-12796.

Evans PN, Parks DH, Chadwick GL, Robbins SJ, Orphan VJ, Golding SD, Tyson GW (2015) Methane metabolism in the
 archaeal phylum Bathyarchaeota revealed by genome-centric metagenomics. *Science*, 350, 434-438.

- Feistel R, Weinreben S, Wolf H et al. (2010) Density and absolute salinity of the Baltic Sea 2006–2009. *Ocean Science*, 6, 3-24.
- 570 Fortney N, He S, Converse B, Beard B, Johnson C, Boyd ES, Roden E (2016) Microbial Fe (III) oxide reduction potential in Chocolate Pots hot spring, Yellowstone National Park. *Geobiology*, 14, 255-275.
- Fossing H, Jørgensen BB (1989) Measurement of bacterial sulfate reduction in sediments: evaluation of a single-step chromium reduction method. *Biogeochemistry*, 8, 205-222.
- Franz D, Koebisch F, Larmanou E, Augustin J, Sachs T (2016) High net CO₂ and CH₄ release at a eutrophic shallow lake on a formerly drained fen. *Biogeosciences*, 13, 3051-3070.
- 575 Habicht KS, Canfield DE (1997) Sulfur isotope fractionation during bacterial sulfate reduction in organic-rich sediments. *Geochimica et Cosmochimica Acta*, 61, 5351-5361.
- Hahn J, Köhler S, Glatzel S, Jurasinski G (2015) Methane exchange in a coastal fen in the first year after flooding-a systems shift. *PloS one*, 10, e0140657.
- 580 Hartmann M, Nielsen H (2012) $\delta^{34}\text{S}$ values in recent sea sediments and their significance using several sediment profiles from the western Baltic Sea. *Isotopes in environmental and health studies*, 48, 7-32.
- Hemes KS, Chamberlain SD, Eichelmann E, Knox SH, Baldocchi DD (2018) A biogeochemical compromise: The high methane cost of sequestering carbon in restored wetlands. *Geophysical Research Letters*.
- Herlemann DP, Labrenz M, Jürgens K, Bertilsson S, Wanek JJ, Andersson AF (2011) Transitions in bacterial communities along the 2000 km salinity gradient of the Baltic Sea. *The ISME journal*, 5, 1571.
- 585 Holm GO, Perez BC, Mcwhorter DE, Krauss KW, Johnson DJ, Raynie RC, Killebrew CJ (2016) Ecosystem level methane fluxes from tidal freshwater and brackish marshes of the Mississippi River Delta: Implications for coastal wetland carbon projects. *Wetlands*, 36, 401-413.
- Iversen N, Jørgensen BB (1985) Anaerobic methane oxidation rates at the sulfate-methane transition in marine sediments from Kattegat and Skagerrak (Denmark) 1. *Limnology and Oceanography*, 30, 944-955.
- 590 Kaplan I, Rittenberg S (1964) Microbiological fractionation of sulphur isotopes. *Microbiology*, 34, 195-212.
- Karstens S, Buczek U, Jurasinski G, Peticzka R, Glatzel S (2016) Impact of adjacent land use on coastal wetland sediments. *Science of the Total Environment*, 550, 337-348.
- King GM, Wiebe W (1980) Regulation of sulfate concentrations and methanogenesis in salt marsh soils. *Estuarine and Coastal Marine Science*, 10, 215-223.
- 595 Koch M, Koebisch F, Hahn J, Jurasinski G (2017) From meadow to shallow lake: Monitoring secondary succession in a coastal fen after rewetting by flooding based on aerial imagery and plot data. *Mires & Peat*, 19.
- Koebisch F, Glatzel S, Jurasinski G (2013) Vegetation controls methane emissions in a coastal brackish fen. *Wetlands ecology and management*, 21, 323-337.

- 600 Koebsch F, Jurasinski G, Koch M, Hofmann J, Glatzel S (2015) Controls for multi-scale temporal variation in ecosystem methane exchange during the growing season of a permanently inundated fen. *Agricultural and Forest Meteorology*, 204, 94-105.
- Kornel BE, Werner RA, Gehre M (1999) Standardization for oxygen isotope ratio measurement—still an unsolved problem. *Rapid Communications in Mass Spectrometry*, 13, 1248-1251.
- 605 Kowalski N, Dellwig O, Beck M et al. (2012) A comparative study of manganese dynamics in the water column and sediments of intertidal systems of the North Sea. *Estuarine, Coastal and Shelf Science*, 100, 3-17.
- Kwieceński B (1965) The sulfate content of Baltic water and its relation to the chlorinity. In: *Deep Sea Research and Oceanographic Abstracts*. pp Page, Elsevier.
- Lapham L, Proctor L, Chanton J (1999) Using respiration rates and stable carbon isotopes to monitor the biodegradation of oil emulsion by marine benthic bacteria. *Environmental science & technology*, 33, 2035-2039.
- 610 Lovley DR, Klug MJ (1983) Sulfate reducers can outcompete methanogens at freshwater sulfate concentrations. *Applied and Environmental Microbiology*, 45, 187-192.
- Mann JL, Vocke Jr RD, Kelly WR (2009) Revised $\delta^{34}\text{S}$ reference values for IAEA sulfur isotope reference materials S-2 and S-3. *Rapid Communications in Mass Spectrometry: An International Journal Devoted to the Rapid Dissemination of Up-to-the-Minute Research in Mass Spectrometry*, 23, 1116-1124.
- 615 Martens CS, Berner RA (1974) Methane production in the interstitial waters of sulfate-depleted marine sediments. *Science*, 185, 1167-1169.
- Martin M (2011) Cutadapt removes adapter sequences from high-throughput sequencing reads. *EMBnet. journal*, 17, pp. 10-12.
- 620 McDonald D, Price MN, Goodrich J et al. (2012) An improved Greengenes taxonomy with explicit ranks for ecological and evolutionary analyses of bacteria and archaea. *The ISME journal*, 6, 610.
- Miegel K, Graeff T, Selle B, Salzmann T, Franck C, Bronstert A (2016) Untersuchung eines renaturierten Niedermoores an der mecklenburgischen Ostseeküste—Teil I: Systembeschreibung und hydrologische Grundcharakterisierung. *HyWa*. doi, 10, 5675.
- 625 Miller RL (2011) Carbon gas fluxes in re-established wetlands on organic soils differ relative to plant community and hydrology. *Wetlands*, 31, 1055-1066.
- Oremland RS, Polcin S (1982) Methanogenesis and sulfate reduction: competitive and noncompetitive substrates in estuarine sediments. *Applied and Environmental Microbiology*, 44, 1270-1276.
- Postma D, Jakobsen R (1996) Redox zonation: equilibrium constraints on the Fe (III)/SO₄-reduction interface. *Geochimica et Cosmochimica Acta*, 60, 3169-3175.
- 630 Price FT, Shieh Y (1979) Fractionation of sulfur isotopes during laboratory synthesis of pyrite at low temperatures. *Chemical Geology*, 27, 245-253.

- Raghoebarsing AA, Pol A, Van De Pas-Schoonen KT et al. (2006) A microbial consortium couples anaerobic methane oxidation to denitrification. *Nature*, 440, 918.
- 635 Sánchez-Arcilla A, García-León M, Gracia V, Devoy R, Stanica A, Gault J (2016) Managing coastal environments under climate change: Pathways to adaptation. *Science of the Total Environment*, 572, 1336-1352.
- Schönheit P, Kristjansson JK, Thauer RK (1982) Kinetic mechanism for the ability of sulfate reducers to out-compete methanogens for acetate. *Archives of Microbiology*, 132, 285-288.
- Segarra K, Schubotz F, Samarkin V, Yoshinaga M, Hinrichs K, Joye S (2015) High rates of anaerobic methane oxidation in
640 freshwater wetlands reduce potential atmospheric methane emissions. *Nature communications*, 6, 7477.
- Segarra KE, Comerford C, Slaughter J, Joye SB (2013) Impact of electron acceptor availability on the anaerobic oxidation of methane in coastal freshwater and brackish wetland sediments. *Geochimica et Cosmochimica Acta*, 115, 15-30.
- Segers R, Kengen S (1998) Methane production as a function of anaerobic carbon mineralization: a process model. *Soil Biology and Biochemistry*, 30, 1107-1117.
- 645 Selle B, Graeff T, Salzmann T, Oswald SE, Walther M, Miegel K (2016) Untersuchung eines renaturierten Mooreinzugsgebiets an der mecklenburgischen Ostseeküste–Teil II: Salzdynamik und Wasserhaushalt.
- Sim MS, Bosak T, Ono S (2011) Large sulfur isotope fractionation does not require disproportionation. *Science*, 333, 74-77.
- Stookey LL (1970) Ferrozine---a new spectrophotometric reagent for iron. *Analytical chemistry*, 42, 779-781.
- Takai K, Horikoshi K (2000) Rapid detection and quantification of members of the archaeal community by quantitative PCR
650 using fluorogenic probes. *Applied and Environmental Microbiology*, 66, 5066-5072.
- Vanselow-Algan M, Schmidt S, Greven M, Fiencke C, Kutzbach L, Pfeiffer E-M (2015) High methane emissions dominated annual greenhouse gas balances 30 years after bog rewetting. *Biogeosciences*, 12, 4361-4371.
- Virtanen S, Simojoki A, Hartikainen H, Yli-Halla M (2014) Response of pore water Al, Fe and S concentrations to waterlogging in a boreal acid sulphate soil. *Science of the Total Environment*, 485, 130-142.
- 655 Voigtländer U, Schmidt J, Scheller W (1996) Pflege-und Entwicklungsplan NSG Heiligensee und Hütelmoor.
- Wasmund K, Cooper M, Schreiber L et al. (2016) Single-cell genome and group-specific *dsrAB* sequencing implicate marine members of the class Dehalococcoidia (Phylum Chloroflexi) in Sulfur Cycling. *MBio*, 7, e00266-00216.
- Wen X, Unger V, Jurasinski G et al. (2018) Predominance of methanogens over methanotrophs in rewetted fens characterized by high methane emissions. *Biogeosciences*, 15, 6519-6536.
- 660 Whalen S (2005) Biogeochemistry of methane exchange between natural wetlands and the atmosphere. *Environmental Engineering Science*, 22, 73-94.
- Whiticar MJ, Faber E, Schoell M (1986) Biogenic methane formation in marine and freshwater environments: CO₂ reduction vs. acetate fermentation— isotope evidence. *Geochimica et Cosmochimica Acta*, 50, 693-709.
- Wilhelm E, Battino R, Wilcock RJ (1977) Low-pressure solubility of gases in liquid water. *Chemical reviews*, 77, 219-262.
- 665 Wilson D, Alm J, Laine J, Byrne KA, Farrell EP, Tuittila ES (2009) Rewetting of cutaway peatlands: are we re-creating hot spots of methane emissions? *Restoration ecology*, 17, 796-806.

670

Winde V, Böttcher M, Escher P, Böning P, Beck M, Liebezeit G, Schneider B (2014) Tidal and spatial variations of $\delta^{13}C$ and aquatic chemistry in a temperate tidal basin during winter time. *Journal of Marine Systems*, 129, 396-404.

Zhang Z, Zimmermann NE, Stenke A et al. (2017) Emerging role of wetland methane emissions in driving 21st century climate change. *Proceedings of the National Academy of Sciences*, 201618765.

Zhao Q, Bai J, Huang L, Gu B, Lu Q, Gao Z (2016) A review of methodologies and success indicators for coastal wetland restoration. *Ecological indicators*, 60, 442-452.

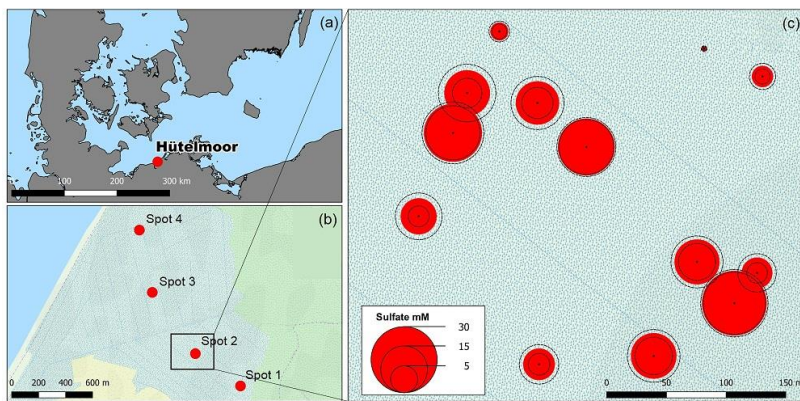


Figure 1: (a) The study site Hütelmoor is located directly at the south-western Baltic coast at an altitude between -0.2 and +0.2 m above sea level. In its pristine state, the site was exposed to episodic brackish water intrusion by storm surges. (b) Profiles of sediments and pore waters were taken along a transect with 300-1,500 m distance to the coast line. Deviations of the transect from the straight normal to the Baltic coast-line arose due to the restricted accessibility of the site. (c) A former study located close to spot 2 in the center of the current sampling transect revealed high pore water sulfate concentrations in 30-60 cm below surface with annual means up to 24 ± 3 mM (red circles indicate annual means while dashed circle lines represent the standard deviation over the year). Map data copyrighted OpenStreetMap contributors and available from <http://www.openstreetmap.org>.

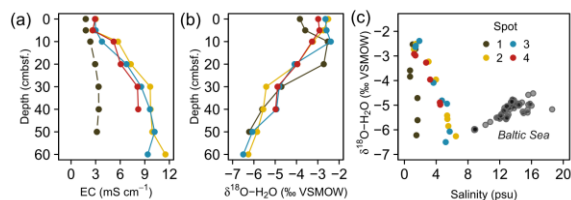


Figure 2: Depth distributions of electrical conductivity (EC, a) and pore water O isotope composition (b). Fig. 2c depicts a scatter plot of (a and b) and scatter plots (c) of electrical conductivity (EC) respectively. Salinity and pore water O isotope composition and salinity. Filled Grey transparent dots in Fig. 2c represent a common positive $\delta^{18}\text{O}\text{-H}_2\text{O}$ vs. salinity relationship derived from a sampling campaign of Baltic Sea surface water (unpublished).

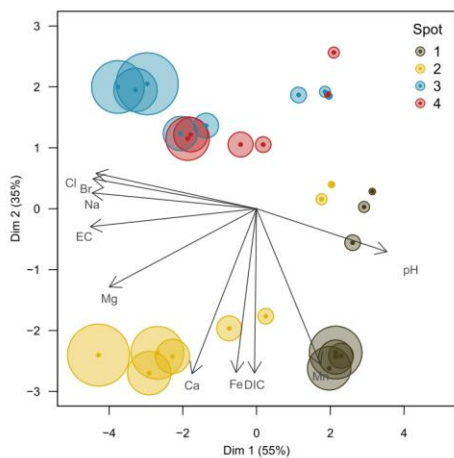
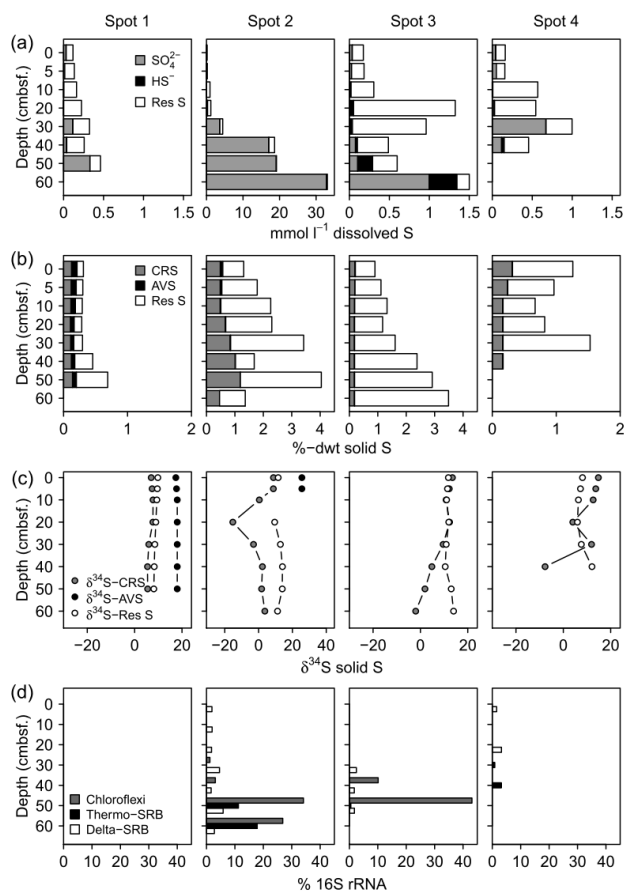


Figure 3: Principal component biplot of pore water geochemical patterns within the peatland. Different colors indicate different sampling locations within the brackish-freshwater continuum with spot 1 closest to the freshwater catchment and spot 4 closest to the Baltic Sea. The size of the data points scales with sampling depth (smallest points indicate surface patterns, largest points indicate pore water composition in 60 cm depth).



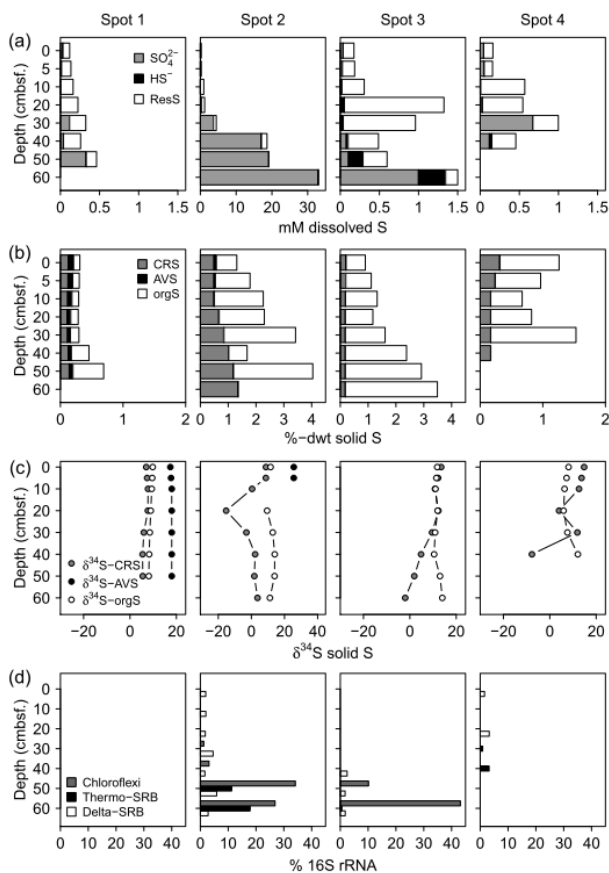


Figure 4: Speciation of dissolved (a) and solid (b) S compounds, S isotope composition of solid S compounds (c), and average relative abundances of sulfate reducing bacteria (SRB, d). Sufficient SO₄²⁻ for δ³⁴S and δ¹⁸O ratio analysis was only available at the bottom of spot 2 and 3 and are displayed in Fig. 6a. The Residuals for dissolved S (ResS in Fig. 4a) and solid S refers to a non-specified S fractions evolving resulting from the difference between a total dissolved S, H₂S and SO₄²⁻ quantity and specified S compounds. The ResS dissolved residual S fraction is most likely composed of dissolved organic S, polysulfides, and S intermediates. The solid residual S fraction is suggested to present primarily organic-bond S. Specified solid S fractions (Fig. 4b) include iron monosulfide operationally defined as acid volatile sulfur (AVS), and pyrite extracted as chromium-reducible sulfur (CRS), and a residual fraction suggested to consist primarily of organic S (orgS). δ³⁴S at AVS could only be measured at spot 1 and the top of spot 2. SRB were extracted from two replicates of 16S rRNA bacterial community sequencing and are assigned to the Deltaproteobacteria (Delta-SRB) and the Nitrospirae phylum (Genus Thermodesulfobionaceae – Thermo-SRB). Chloroflexi Dehalococcoides (Chloroflexi) have not been assigned to SRB in the classical sense, however, they could be potentially involved in S metabolism (Wasmund et al., 2016). Note different x axis scales.

Formatiert: Tiefgestellt

Formatiert: Tiefgestellt

Formatiert: Hochgestellt

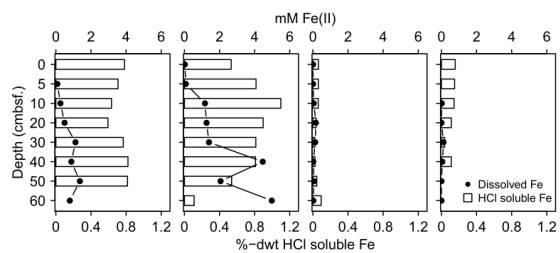


Figure 5: Mobile Fe species. Available solid iron was extracted as HCl soluble iron from the sediment matrix and is composed of iron mono-sulfide and non-sulfidized ferric Fe.

715

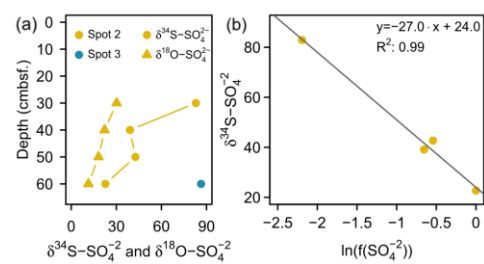
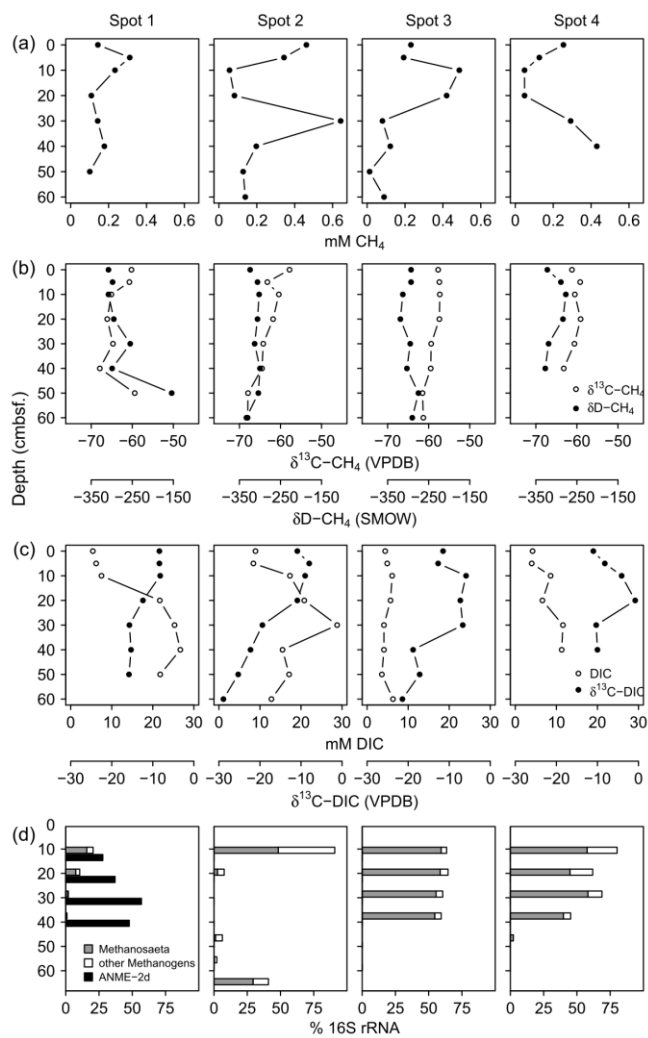


Figure 6: (a) S and O isotope composition of sulfate. Sufficient SO_4^{2-} for $\delta^{34}\text{S}$ and $\delta^{18}\text{O}$ ratio analysis was only available at the bottom of spot 2 and spot 3 (here only $\delta^{34}\text{S}$). (b) Rayleigh plot for measured SO_4^{2-} depletion at spot 2.



720 **Figure 7: Concentration patterns and isotope ratios for CH_4 (a, b) and DIC (c), as well as average relative abundances of methanogens and methanotrophs (d).**

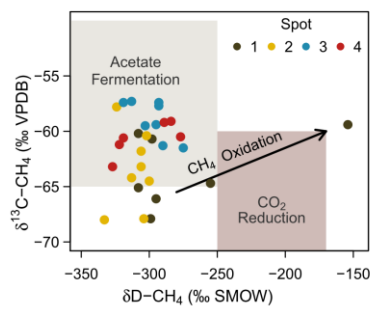


Figure 8: Projection of the CH₄ stable isotope composition to differentiate dominating methanogenic pathways and methanotrophy. Isotope thresholds to confine methanogenic pathways base on Whiticar et al. (1986). The concurrent increase in $\delta^{13}\text{C-CH}_4$ and $\delta\text{D-CH}_4$ values at spot 1 suggests a downwards shift towards increasing CO₂ reduction or CH₄ oxidation rates at depth.